MINISTRY OF SUPPLY

AERONAUTICAL RESEARCH COUNCIL
REPORTS AND MEMORANDA

A Method of Performance Estimation
for Axial-Flow Turbines

By

D. G. AINLEY and G. C. R. MATHIESON

LONDON : HER MAJESTY'S STATIONERY OFFICE

1957

NINE SHILLINGS NET

A Method of Performance Estimation for Axial-Flow Turbines

By

D. G. AINLEY and G. C. R. MATHIESON

COMMUNICATED BY THE PRINCIPAL DIRECTOR OF SCIENTIFIC RESEARCH (AIR),
MINISTRY OF SUPPLY

Summary.—A method for calculation of the performance of conventional axial-flow turbines is presented. It makes use of data derived from the analysis of a large number of turbine tests and other associated test work reported elsewhere. The method enables the performance of a turbine to be calculated over a wide part of its full operating range. It is estimated that the tolerance on the absolute values of gas mass flow and peak efficiency will be in the region of $\pm 2 \cdot 0$ per cent for efficiency and ± 3 per cent for gas mass flow on present day types of turbine.

The method is illustrated by a worked example.

1. *Introduction.*—The estimation of the performance of a gas-turbine stage under different conditions of speed and pressure ratio has until recently been hampered by lack of reliable data regarding the pressure losses and gas deflections through rows of turbine blading. Information from cascade tests, giving the two-dimensional performance of blade sections, is not enough. The three-dimensional effects in a turbine are so powerful that unless they can be estimated with a fair degree of accuracy, prediction of the performance of blading fitted in a turbine is largely reduced to the level of guess-work. The construction and operation of an increasing number of rigs for the detail testing of gas turbines has made available a stock of test calibrations from which some useful experimental data has been extracted by analysis. Ref. 1 gives an account of the work which has been carried out at the National Gas Turbine Establishment on this analysis and the conclusions which have been drawn from it.

This present report gives a method of estimating the performance of a turbine, making use of the data derived in that analysis. The method proposed applies to axial-flow turbines only. Some of the basic data presented here will be of use in the performance estimation of some types of radial-flow turbines (such as the Ljungström type) but the three-dimensional flow picture will be different as between the axial and radial types, and so the method cannot be used directly for radial-flow machines.

2. *Application of the Method.*—The procedure adopted in this method can be split conveniently into two parts. The first is the determination of the characteristics of pressure loss and gas efflux angle for each blade row in the turbine under a wide range of inlet conditions. The second is to take a fixed set of conditions at inlet to the turbine and a given turbine speed and to follow

the course of a fixed mass of the gas from one blade row to the next, calculating the new gas conditions at each step, so building up a complete picture of the flow at all points for the given initial conditions. Then from the final picture, the necessary information such as gas angles, stage and overall pressure ratios, stage and overall efficiencies and the gas mass flow can be extracted.

The procedure of the second part must be repeated for several sets of initial conditions with the same turbine speed and further points on a constant-speed characteristic curve can be constructed. Another speed may then be selected and the calculations of the second part repeated to give a second constant-speed curve. This may be repeated for further constant-speed curves but, to save calculation, it is only necessary in many instances to calculate the performance at two turbine speeds. A method is suggested of interpolating the characteristics at intermediate speeds.

Since the turbine outlet conditions are not initially fixed, but determined by the final result of a row-by-row progression, the direct calculation of a characteristic curve at constant pressure ratio is not possible. If such characteristics are required they have to be obtained by interpolation between series of constant-speed curves.

3. *Limitations of the Method.*—To predict exactly the flow at all points in a system such as a turbine an almost infinite number of variables would ultimately have to be considered. In contrast to this, to achieve simplicity in a method of prediction the number of variables must be reduced to a minimum. Thus any working method finally arrived at must be a compromise between simplicity on the one hand and accuracy on the other.

In the present method only those variables which calculation or statistical experimental evidence has so far proved to be essential to achieve a final tolerance of about $\pm 2 \cdot 0$ per cent in efficiency and flow have been employed. This tolerance is about the same magnitude as that which must be allowed in interpreting most current experimental data and higher accuracy scarcely seems possible at the present time.

A major simplification employed throughout the following treatment is the widely adopted one of considering the flow path through each stage at one diameter only—this diameter being termed the ' reference diameter.' The reference diameter selected in each stage is the arithmetic mean of the rotor and stator row inner and outer diameters (*see* Fig. 2). In adopting this procedure it is assumed that in any one cross-sectional plane of the flow between adjacent blade rows the total pressure, total temperature, and axial velocity are equal at all points. Such an assumption, though often widely divorced from fact, may be expected to yield correct overall characteristics of a stage if the gas efflux angles and pressure loss coefficients used for each blade row at the reference diameter in the calculation are equal to the momentum mean values over the entire cross-sectional plane which would be determined by a flow exploration in the actual turbine. The accuracy of the performance calculation rests entirely upon the accuracy with which these mean loss coefficients and gas flow angles for each blade row may be predicted.

The present method owes its accuracy to the fact that the loss coefficient and gas angle data have been derived largely from overall tests on a variety of turbine stages (Ref. 1). At the same time this sets a limitation to the method since the data so obtained applies primarily to blades having a ' conventional ' (Ref. 1) profile shape and the quoted accuracy cannot therefore be guaranteed for widely different profile shapes. However, the data should apply to most blade designs in current use in gas and steam turbines in this country and the U.S.A. so that calculations made in accordance with the present treatment should prove to be of wide use.

Since the present treatment allows loss coefficients and efflux angles in any blade row to vary with gas flow conditions, such as incidence and Mach number, it may be expected to give greater accuracy over a wide range of operating conditions in a turbine than earlier and simpler methods (*e.g.*, Refs. 2 and 3) in which constant loss coefficients and gas efflux angles in blade rows have been assumed.

2

4. *Notation and Convention of Signs.*—The notation and convention of signs for the gas-velocity triangles in each stage is similar to that used in Ref. 4 and follows directly from that already established in axial-compressor theory in this country. A complete list of symbols and a note on the convention of signs is given in Appendix I ; the velocity triangle notation and sign convention is further illustrated in Fig. 1 ; critical dimensions used to define blade form are further illustrated in Fig. 3. Fig. 2 illustrates the choice of the reference diameter and the reference stations between adjacent blades together with the dimensions used to define annulus areas at the reference stations, blade height, and tip clearances.

In each stage the suffices adopted for absolute and relative pressures and temperatures at each station are the same as the suffices used for gas angles and velocities in the relevant velocity triangles. These suffices repeat themselves from stage to stage so that care must be taken when setting out the calculation to ensure that pressures calculated at any station are associated with the correct stage.

In section 5 (dealing with the estimation of loss coefficients and gas angles) and in Fig. 3 (illustrating critical dimensions used to specify blade shape) it should be noted that the notation relates to a rotor row. This has been done for convenience since this same notation was used in Ref. 1 (dealing with the derivation of the data). The procedure for determining the loss coefficients and gas outlet angles on a stator row is precisely similar—suffices $_3$ and $_0$ (or $_i$ and $_0$ if it is a first-stage stator) merely being substituted for $_1$ and $_2$ respectively.

5. *Determination of the Variation of Gas Deflection and Total-Pressure Loss in a Row of Blades with Incidence and Mach Number.*—The derivation of the pressure losses and gas efflux angles for each blade row follows directly from the analysis described at length in Ref. 1: The blade sections at the reference diameter on each row are treated as the reference sections used for predicting the aerodynamic characteristics of each row.

Throughout the succeeding treatment the following assumptions are made :

(i) The pressure-loss coefficients in each blade row defined by the ratio (inlet total pressure — outlet total pressure)/(outlet total pressure — outlet static pressure), are not influenced by the gas Mach numbers.

(ii) The gas outlet angles from a blade row are not influenced by the gas incidence angle.

The assumption that the loss coefficient is uninfluenced by gas Mach number is unlikely to lead to appreciable error unless the blades have a high degree of curvature on the upper surface near the trailing edge. Since such blades have been shown to have high losses when the outlet Mach number approaches unity such blades are unlikely to be used in practice at high Mach numbers.

The assumption that outlet angle remains independent of incidence does not accord precisely with fact but will lead to very little error over the efficient operating range of a turbine.

Neither of these assumptions are absolutely essential to the method of calculation propounded in section 6. They are introduced primarily because they reduce the amount of trial and error necessary in the calculation. If in any calculation it is felt desirable to take account of variation of loss coefficient and gas angle with Mach number and incidence respectively the general methods outlined in section 6 may still be used.

The effect of Reynolds number is discussed in section 8.

5.1. *Derivation of the Gas Outlet Angle from a Blade Row.*—Following the recommendations made in Ref. 1 it is assumed that gas outlet angle from any row remains constant over the gas outlet Mach number range $0 \cdot 5 > M_2 > 0$ and given over this range by :

$$\alpha_2 = \alpha_2{}^* - 4(s/e) \quad \text{..} \quad \text{..} \quad \text{..} \quad \text{..} \quad \text{..} \quad \text{..} \quad \text{..} \quad \text{..} \quad (1)$$

where $\qquad \alpha_2{}^* = f\,(\cos^{-1} o/s),\ see$ Fig. 5

3

AI

e is the mean radius curvature of the upper surface of the blade profile between the passage throat and the trailing edge (*see* Fig. 3).

s is the blade pitch.

At a gas outlet Mach number of unity it is assumed that the outlet angle is given by :

$$\alpha_2 = -\cos^{-1} A_t / A_{n\,2} \qquad \qquad \qquad \qquad \qquad \qquad \qquad (2)$$

where A_t is the passage throat area

A_{n2} is the annulus area in reference plane downstream of the blade row.

If the annulus walls at the ends of the blades are flared the throat area may be approximately expressed by an empirical formula :

$$A_t = (o/s)_{m/d} \, [5A_{n\,2} + A_{n\,0}]/6 \qquad \qquad \qquad \qquad \qquad \qquad (3)$$

where $A_{n\,0}$ is the annulus area in reference plane upstream of row

$A_{n\,2}$ is the annulus area in reference plane downstream of row.

Between $M_2 = 0\cdot5$ and $M_2 = 1\cdot0$ a linear variation of α_2 may be assumed with reasonable accuracy. Alternatively a smooth curve with a point of inflection at $M_2 = 0\cdot75$ may be arbitrarily drawn similar to those shown in Fig. 17. A variation of this latter form will occasionally be found more convenient in practice since it will be found to ease a trial and error step required in the calculation when the flow approaches the choking flow (*see* sections 6.1 and 6.3 later).

The outlet angles as deduced in the above paragraphs apply to blades having zero tip or shroud clearance. If a finite tip or shroud clearance exists then a small portion of the flow passes through the row with little or no deflection and the momentum mean outlet angle is thereby reduced slightly.

At low Mach numbers, if α_2 is the mean outlet angle from a row having a small tip clearance and α_2' is the angle deduced ($M_2 < 0\cdot5$) for zero clearance then α_2 is given approximately by :

$$\alpha_2 = \tan^{-1} \{[1 - X(k/h)(\cos\beta_1/\cos\alpha_2')]\tan\alpha_2' + X(k/h)(\cos\beta_1/\cos\alpha_2')\tan\beta_1\} \qquad (4)$$

where $X = 1\cdot35$ for radial tip clearance

or $= 0\cdot70$ for simple shrouded blade.

For complex shroud bands the expression $(k/h)(\cos\beta_1/\cos\alpha_2')$ may be replaced by w/W where w is the estimate leakage flow round the band and W is the total flow. In this case $X = 1\cdot35$.

At $M_2 = 1\cdot0$ the angle is deduced from equation (2) by allowing for the tip clearance area in the evaluation of throat area. Thus if A_t' is passage throat area when the clearance is zero then $A_t = A_t'[1 - (k/h)] + A_k$ where A_k is the flow area in the clearance space, *e.g.*, if the tip diameter is D inches and the radial tip clearance is k inches then $A_k = \pi Dk$ sq in.

If the row has a shroud then the throat area should be $A_t = A_t' + A_k$.

5.2. *Derivation of Pressure Losses in a Blade Row.*—The pressure loss is subdivided into three components, namely (i) profile loss (ii) secondary loss and (iii) tip or shroud clearance loss.

(i) *Profile Loss.*—Firstly profile loss is determined at zero incidence. The stalling incidence of the blade row is then determined, stalling incidence being defined as the incidence at which profile loss is twice the loss at zero incidence. Profile losses at incidences other than zero are then obtained from the assumption that the ratio of profile loss at any incidence to profile loss at zero incidence, $Y_p/Y_{p(i=0)}$, is a function of the ratio of incidence to stalling incidence, i/i_s. This relationship (derived in Ref. 1) is plotted in Fig. 6.

4

Profile-loss coefficient at zero incidence is assumed to be a function of α_2, β_1/α_2, s/c, and t/c and is given by :

$$Y_{p(i=0)} = \left\{ Y_{p(\beta_1=0)} + (\beta_1/\alpha_2)^2 [Y_{p(\beta_1=-\alpha_2)} - Y_{p(\beta_1=0)}] \right\} \left(\frac{t/c}{0\cdot 2} \right)^{-\beta_1/\alpha_2} \qquad .. \qquad .. \qquad (5)$$

where, $Y_{p(\beta_1=0)}$ is the profile-loss coefficient of a blade having $\beta_1 = 0$ and same α_2 and s/c as the actual blade (Fig. 4).

         $Y_{p(\beta_1=-\alpha_2)}$ is the profile-loss coefficient of a blade having $\beta_1 = -\alpha_2$ and same α_2 and s/c as the actual blade (Fig. 4).

On impulse or nearly impulse blades the use of equation (5) should be restricted to $0\cdot 15 < t/c < 0\cdot 25$. If the actual blade has t/c greater or less than the limits quoted then the loss should be taken as equal to a blade having t/c either $0\cdot 25$ or $0\cdot 15$ respectively (Ref. 1).

Stalling incidence is approximately a function of α_2, β_1/α_2, and s/c. Fig. 7 enables stalling incidences of a wide range of blades having $s/c = 0\cdot 75$ to be determined and also shows the variation of stalling incidence and gas outlet angle with s/c. The procedure for determining stalling incidence for a given blade for which α_2, β_1, and s/c is known is then as follows :

(a) From Fig. 7 find $\alpha_2(s/c = 0\cdot 75)/\alpha_2$ for given value of s/c and hence find $\alpha_2(s/c = 0\cdot 75)$.

(b) Determine $\beta_1/\alpha_2(s/c = 0\cdot 75)$ and from Fig. 7b find $i_s(s/c = 0\cdot 75)$.

(c) From Fig. 7a find Δi_s for actual value of s/c and hence determined i_s from :
$$i_s = i_s(s/c = 0\cdot 75) + \Delta i_s.$$

This value of stalling incidence is, of course, only approximate, but the accuracy is considered sufficient for the present purposes.

Having now determined i_s and $Y_{p(i=0)}$ the profile-loss coefficients over a wide range of incidence can be deduced from Fig. 6.

(ii) *Secondary and Tip Clearance Loss.*—It has been demonstrated in Ref. 1 that secondary losses may be conveniently expressed by an equation of the form :
$$C_{Ds} = \lambda C_L^2/(s/c)$$
where λ is dependent primarily upon the degree of acceleration imparted to the gas as it flows through the blade row. Similarly it was shown that tip clearance losses may be expressed by :
$$C_{Dk} = B(k/h)C_L^2/(s/c)$$
where B is a constant.

Since the equation for secondary and tip clearance losses are similar in form it is convenient to treat them simultaneously. Thus, converting the drag coefficients into the more convenient loss coefficients[1], we may derive an expression for the sum of the secondary and tip clearance losses :—

$$Y_s + Y_k = [\lambda + B(k/h)][C_L/(s/c)]^2[\cos^2 \alpha_2/\cos^3 \alpha_m] \qquad .. \qquad .. \qquad .. \qquad .. \qquad (6)$$

where $\lambda = f\left\{(A_2/A_1)^2/(1 + I.D./O.D.)\right\}$, *see* Fig. 8

         $A_1 = A_{n0} \cos \beta_1$

         $A_2 = A_{n2} \cos \alpha_2$

     $C_L/(s/c) = 2(\tan \alpha_1 - \tan \alpha_2) \cos \alpha_m$

         $\alpha_m = \tan^{-1} [(\tan \alpha_1 + \tan \alpha_2)/2]$

         $B = 0\cdot 5$ for row with radial tip clearance or $0\cdot 25$ for row with shroud seal.

Equation (6) may be used to find the secondary and tip clearance loss for a wide range of gas inlet angles. The variations of these losses with gas inlet angle to a blade row at large positive and negative incidences is uncertain but reasonable correlation of test and calculated turbine

5

performance has been obtained by restricting the use of equation (6) to $-1 \cdot 5 \leqslant i/i_s \leqslant 1 \cdot 0$ At values of $i/i_s > 1 \cdot 0$ the secondary and clearance loss coefficients should be assumed constant and equal to the value when $i/i_s = 1 \cdot 0$. Similarly when $i/i_s < -1 \cdot 5$ secondary and clearance loss is assumed to remain constant and equal to the value at $i/i_s = -1 \cdot 5$.

(iii) *Effect of Trailing-Edge Thickness on Blade Loss.*—The preceding pressure loss coefficients apply to ' conventional ' blades having a trailing-edge thickness, t_e, roughly equal to 2 per cent of the blade pitch. Reeman[5] has shown theoretically that trailing-edge thickness can markedly influence the loss and it was further indicated in Ref. 1 that theoretical estimates of the effect of trailing-edge thickness based on total loss coefficients have compared favourably with observations made on turbine and engine tests. If the ratio of trailing-edge thickness to blade pitch, t_e/s, differs from $0 \cdot 02$ then the total loss coefficients deduced from the previous sections should be corrected by a multiplication factor plotted in Fig. 9, this factor being derived from the previous mentioned references.

6. *Performance of a Turbine Stage (unchoked).*—Having determined the characteristics of each individual row of blades it is now possible to proceed with the calculation of the performance of the complete turbine. At this point the following information should have been determined :

(a) The reference diameter of each stage

(b) Annulus areas at the reference stations mid-way in the axial clearance spaces between adjacent blade rows

(c) Estimated variation of gas outlet angle with gas outlet Mach number at the reference diameter of each row

(d) Estimated variation of the total loss coefficient, Y_t, with incidence for each row.

An inlet mass flow, inlet pressure, and inlet temperature are now arbitrarily selected and at a fixed turbine speed the course of the chosen mass of flow is followed from row to row, gas temperature and pressure being determined at the entry and exit of each row. K_p and γ are assumed to remain constant throughout expansion of the gas through the turbine. The process will be described in detail for one stage. Further stages should be treated in a similar fashion.

For accomplishing the calculations it is essential to have at hand a set of curves relating the parameters $V/\sqrt{T}$ and M with the non-dimensional flow quantity $W\sqrt{T}/AP$, these curves being calculated for isentropic expansion of the gas from the stagnation pressure, P, and stagnation temperature, T. The relationships between these parameters have been calculated for $\gamma = 1 \cdot 3330$, $K_p = 12,300$ ft/pdl/deg C., $g = 32 \cdot 173$ ft/sec^2 and are tabulated in Appendix IV. Further relationships between non-dimensional flow parameters are also required and are described later in section 6.1, and plotted in Figs. 10, 11 and 12. It is important that these latter relationships should be calculated for the same values of γ, K_p and g as the former. Since the computation of these curves for various values of K_p and γ is very laborious it is recommended that all performance calculations on turbines should be made using some arbitrarily defined standard values of gas properties. If the turbine characteristics are required for other values of K_p and γ the final characteristics obtained using the ' standard ' values should be corrected by one of the simple methods described in Ref. 4.

6.1. *Determination of Gas Flow Conditions at Outlet from a Nozzle Row.*—Suitable turbine entry values of inlet temperature, inlet pressure, inlet gas flow direction (usually axial at entry to the first nozzle) should be decided and a first value for gas mass flow arbitrarily selected. If the nozzle row is preceded by other turbine stages then, of course, these inlet conditions will be already determined.

The pressure loss coefficient for the row is determined by the incidence, and the gas outlet angle is a known function of outlet Mach number. Since the pressure loss coefficient for the nozzle row is defined as $(P_i - P_o)/(P_o - p_{so})$ it is seen that both the absolute pressure loss $(P_i - P_o)$ and gas outlet angle depend upon the outlet conditions from the row which are as

yet unknown. At first sight this presents a problem which must be solved by trial and error, *i.e.*, arbitrarily selecting outlet conditions (M_o) until conditions are found which satisfy the requirement of flow continuity. This trial and error process may be nearly eliminated as shown in the following paragraphs.

If a blade row was assumed for the moment to have a constant outlet angle and a constant loss coefficient at all outlet Mach numbers up to unity then it would be found that the non-dimensional inlet mass flow ($W\sqrt{T_i}/A_oP_i$) would increase as M_o increases until it reached a maximum value at a value of M_o slightly less than $1\cdot0$. This phenomenon has been demonstrated in Refs. 6 and 7.

For convenience the value of M_o at which $W\sqrt{T_i}/A_oP_i$ reaches a maximum will be termed the 'critical' outlet Mach number. The actual values of $(W\sqrt{T_i}/A_oP_i)_{max}$, $M_{o\text{ crit}}$, and the ratio of pressure loss to inlet pressure at the critical flow conditions, $(\bar{\omega}/P_i)_{crit}$, all depend upon the value of the loss coefficient, Y_t. Values of $(W\sqrt{T_i}/A_oP_i)_{max}$ and $(\bar{\omega}/P_1)_{crit}$ are plotted in Figs. 10 and 11. Now it is found that over the required range of $M_o(0 < M_o < 1\cdot2)$ and $Y_t(0 \leqslant Y_t < 1\cdot0)$ the ratio of pressure loss to inlet pressure $(\bar{\omega}/P_i)$, can be related to the non-dimensional inlet mass flow $(W\sqrt{T_i}/A_oP_i)$, by a single curve by plotting $(\bar{\omega}/P)/(\bar{\omega}/P)_{crit}$ against $(W\sqrt{T_iA_oP_i})/ (W\sqrt{T_i}/A_oP_i)_{max}$. This relationship is plotted in Fig. 12. Mathematically this relationship is not exactly unique for all values of Y_t but for $0 \leqslant Y_t < 0\cdot1$ the maximum departure from the curve plotted is very small and within 1 per cent. This error is insignificant for the present purposes since a 1 per cent error in blade loss is equivalent to less than $0\cdot2$ per cent in turbine efficiency when the efficiency is in the region of 80 per cent or more.

By employing these relationships a procedure for determining the outlet gas condition from the known inlet conditions may therefore be specified as follows :

(i) Select by conjecture a first approximation to outlet angle, α_o

(ii) From the known mass flow and inlet conditions find $W\sqrt{T_i}/A_oP_i$
[*N.B.*, $A_o = A_{no} \cos \alpha_o$].

(iii) From Figs. 10 and 11 find for the relevant value of Y_t the value of $(W\sqrt{T_i}/A_oP_i)_{max}$ and $(\bar{\omega}/P_i)_{crit}$

(iv) Calculate $(W\sqrt{T_i}/A_oP_i)/(W\sqrt{T_i}/A_oP_i)_{max}$ and hence from Fig. 12 find the corresponding value of $(\bar{\omega}/P_i)/(\bar{\omega}/P_i)_{crit}$

(v) From the above determined values of $(\bar{\omega}/P_i)_{crit}$ and $(\bar{\omega}/P_i)/(\bar{\omega}/P_i)_{crit}$ find $(\bar{\omega}/P_i)$

(vi) Find P_o, given by $P_o = P_i - \bar{\omega}$, and hence determine $W\sqrt{T_o}/A_oP_o$
[*N.B.*, for an uncooled nozzle row $T_o = T_i$].

(vii) From the value of $W\sqrt{T_o}/A_oP_o$ the values of M_o and $V_o/\sqrt{T}$ may be deduced. The table given in Appendix IV should be used for this purpose.

Thus the outlet conditions are determined. If the value of α_o corresponding to the value of M_o found in (vii) differs from the initially assumed value in (i) by more than about $0\cdot2$ deg then the process should be repeated using a second approximation to α_o. With a little experience, however, it is possible to approximate to α_o sufficiently accurately at the outset since its rate of variations with M_o is generally quite small.

6.2. *Determination of Gas Conditions Relative to the Rotor Row at Inlet.*—Knowing the exit gas velocity and flow angle from the nozzle row and the blade speed being known at the reference diameter the gas conditions relative to the inlet of the rotor may be determined.

From the velocity triangles we have the relationships :

$$V_{a1} = V_o \cos \alpha_o \qquad \qquad (7)$$

and $$\tan \alpha_1 = (U/V_{a1}) - \tan \alpha_o \qquad \qquad (8)$$

7

The energy equation gives

$$T = T_s + V^2/2K_p. \quad \dots \quad \dots \quad \dots \quad \dots \quad \dots \quad \dots \quad \dots \quad \dots \tag{9}$$

From equations (7) and (8) the gas inlet angle relative to the rotor, α_1, may be found and hence also the incidence angle. From equation (9) and from the fact that the static temperature at exit from the nozzle is equal to the static temperature relative to the rotor entry (i.e., $T_{so} = T_{s1}$) the total-head temperature relative to the rotor inlet may be found. Thus :

$$T_o = T_{so} + V_o^2/2K_p \quad \dots \quad \dots \quad \dots \quad \dots \quad \dots \quad \dots \quad \dots \tag{10}$$

$$T_1 = T_{s1} + V_1^2/2K_p = T_{so} + V_1^2/2K_p \quad \dots \quad \dots \quad \dots \quad \dots \quad \dots \tag{11}$$

$$T_o - T_1 = (V_o^2 - V_1^2)/2K_p$$

$$= V_o^2 \, (1 - [\cos^2 \alpha_o/\cos^2 \alpha_1])/2K_p. \quad \dots \quad \dots \quad \dots \quad \dots \quad \dots \tag{12}$$

Having found T_1 the total-head pressure relative to the rotor inlet, P_1, may be deduced from

$$P_1/P_o = (T_1/T_o)^{\gamma/\gamma-1} = \{1 - [(T_o - T_1)/T_o]\}^{\gamma/\gamma-1} . \quad \dots \quad \dots \quad \dots \tag{13}$$

Thus the values of P_1, T_1, α_1, and incidence are determined. From the incidence the rotor-loss coefficient may be found.

6.3. *Determination of Gas Conditions Relative to the Rotor at Outlet.*—Since the flow is followed through the rotor along an axial line (*i.e.*, at constant diameter), and since it is assumed that no heat is transferred to or from the blades, there is no change of gas total temperature relative to the row, i.e., $T_2 = T_1$. Knowing the flow conditions relative to the rotor inlet the flow conditions relative to the rotor at the rotor exit may be determined by the same process as was adopted for the nozzle row. Thus :

(i) The value of $W\sqrt{T_1}/A_2 P_1$ is calculated. In this calculation $A_2 = A_{n2} \cos \alpha_2$ and α_2 must be found by making a rough approximation to M_2 and employing the relationship between M_2 and α_2 deduced from section 5.1

(ii) For the value of Y_t found for the rotor row find $(W\sqrt{T_1}/A_2 P_1)_{\max}$ and $(\bar{\omega}/P_1)_{\mathrm{crit}}$ from Figs. 10 and 11

(iii) Calculate the ratio $(W\sqrt{T_1}/A_2 P_1)/(W\sqrt{T_1}/A_2 P_1)_{\max}$ and find corresponding value of $(\bar{\omega}/P_1)/(\bar{\omega}/P_1)_{\mathrm{crit}}$ from Fig. 12

(iv) The value of $\bar{\omega}/P_1$ may then be determined and hence P_2 (given by $P_2 = P_1 - \bar{\omega}$). The magnitude of $W\sqrt{T_2}/A_2 P_2$ may now be calculated and from the table in Appendix IV the corresponding values of $V_2/\sqrt{T_2}$ and M_2 may be found.

As before, if the value of α_2 corresponding to the value of M_2 differs from the value approximated in (i) by more than about $0 \cdot 2$ deg then the process should be repeated using a second approximation to α_2.

6.4. *Determination of Absolute Gas Outlet Conditions from the Rotor.*—From the velocity triangles at the rotor outlet :

$$V_{a2} = V_2 \cos \alpha_2 \quad \dots \quad \dots \quad \dots \quad \dots \quad \dots \quad \dots \quad \dots \quad \dots \tag{14}$$

$$\tan \alpha_3 = (U/V_{a2}) - \tan \alpha_2. \quad \dots \quad \dots \quad \dots \quad \dots \quad \dots \quad \dots \quad \dots \tag{15}$$

From equations (14) and (15) the absolute gas flow angle at rotor exit, α_3, may be found. From the energy equation (equation (9)) the absolute total gas temperature at rotor outlet, T_3, may be derived :

$$T_2 - T_3 = V_2^2[1 - (\cos^2 \alpha_2/\cos^2 \alpha_3)]/2K_p \quad \dots \quad \dots \quad \dots \quad \dots \quad \dots \tag{16}$$

and $\qquad\qquad T_3 = T_2 - (T_2 - T_3) . \quad \dots \quad \dots \quad \dots \quad \dots \quad \dots \quad \dots \quad \dots \tag{17}$

8

The absolute total-head pressure at the rotor outlet may be derived from :

$$P_3/P_2 = (T_3/T_2)^{\gamma/\gamma-1} = \{1 - [(T_2 - T_3)/T_2]\}^{\gamma/\gamma-1}. \qquad .. \qquad .. \qquad .. \qquad .. \qquad (18)$$

6.5. *The Turbine Overall Characteristic.*—The overall stage pressure ratio P_3/P_i, and temperature drop ratio $(T_i - T_3)T_i$ corresponding to the initially selected values of $W\sqrt{T_i}/P_i$ and $N/\sqrt{T_i}$ may now be determined. The overall stage isentropic efficiency is then given by :

$$\eta = [(T_i - T_3)/T_i]/[1 - (P_3/P_i)^{\gamma-1/\gamma}]. \qquad .. \qquad .. \qquad .. \qquad .. \qquad .. \qquad (19)$$

The process described in sections 6.1 to 6.4 may be continued through subsequent stages in multi-stage turbines and both the overall turbine characteristics and also the individual stage characteristics determined for the flow quantity and speed initially selected.

The process must be repeated for several flow quantities at the same values of $N/\sqrt{T_i}$ to construct a constant-speed characteristic, the flows being suitably selected to cover the range over which the characteristic is required. If the calculation is set out in tabular form as shown in Fig. 16 it will be found convenient to estimate the stage characteristics at several flows concurrently.

The entire procedure must be repeated again if the characteristics at more than one speed are required. If the characteristics at two speeds have been calculated then the characteristics at intermediate speeds may usually be interpolated with reasonable accuracy by a method described in Appendix III.

7. *Performance of a Choked or Nearly Choked Stage.*—The procedure outlined in the previous sections may be applied for all flow quantities up to the flow at which the non-dimensional flow parameter $W\sqrt{T_i}/A_oP_i$ in a nozzle row or $W\sqrt{T_1}/A_oP_i$ in a rotor row equals the maximum value possible (this maximum value being dependent upon the loss coefficient for the row as given by Fig. 10).

Choking flow is usually defined as the flow at which the mean gas Mach number in the throat of the blade passage of a row becomes unity. At this point pressure disturbances downstream of the choked row can no longer affect the flow upstream of the row. If the expansion ratio across a turbine is increased beyond the amount required to choke a row the flow Mach number downstream of the choked row will increase to some supersonic value, the gas direction altering slightly to preserve flow continuity. This supersonic expansion will increase as the overall turbine expansion ratio is increased until eventually further choking occurs in another row downstream of the initially choked row. At still higher overall expansion ratios further supersonic expansion will no longer take place downstream of the initially choked row but will commence downstream of the newly choked one. This process can continue until choking occurs in the turbine exhaust ducting. At overall expansion ratios beyond the value at which this occurs the flow conditions in the turbine, and the power output must remain constant (as expressed non-dimensionally).

It has been assumed in the preceding sections that the loss coefficient in any row remains invariant with the outlet Mach number. If the outlet gas angle also remained constant then as mentioned in section 6.1, the non-dimensional flow parameters would rise to a maximum value at an outlet Mach number (the ' critical ' Mach number) less than unity and would then decrease as the outlet Mach number approached unity and the row became fully choked. Turbine test results to the time of writing give no clear indication that such a phenomenon occurs in practice. For the purpose of simplicity in calculation therefore, the following assumptions are made when the outlet Mach number from any row exceeds the critical value :

(a) The flow quantity $W\sqrt{T_i}/P_i$ at the turbine inlet remains constant

(b) The loss coefficient Y_t remains invariant with outlet Mach number

(c) The gas outlet angle from a blade row adjusts itself away from the estimated value at the critical Mach number just sufficiently to preserve constancy of flow.

Thus the variation of flow angle with Mach number for each blade row deduced in section 5.1 is only employed in the calculation up to the critical outlet Mach number. At higher Mach numbers the gas angle used in the calculation will differ from that estimated in section 5.1.

The procedure is demonstrated in detail in the worked example of a turbine performance calculation given in Appendix II.

It is not claimed that the above assumptions are truly representative of what physically occurs in a turbine. The behaviour of the flow in a turbine blade row as the choking expansion ratio is approached and exceeded has not yet been examined in sufficient detail to allow more accurate assumptions to be made. On the other hand the present assumptions lead to simplicity in the calculations and appear to produce final characteristics which compare reasonably well with characteristics acquired experimentally.

8. *Effect of Reynolds Number.*—The greater part of the experimental data from which the approximate working rules for defining loss coefficients and gas angles have been deduced appertain to Reynolds numbers† in the range of 1×10^5 to 3×10^5. Thus any turbine performance as calculated using this present data will correspond to a mean operating Reynolds number of approximately 2×10^5.

The variations with R_e of the components of the pressure losses and also the gas outlet angle from rows of turbine blades are as yet very imperfectly understood. If it is desired to estimate the performance of a turbine operating at mean Reynolds numbers very different from 2×10^5 it is recommended that the performance should first be calculated for a mean Reynolds number of 2×10^5 and an approximate correction then applied to the overall characteristics by assuming that the turbine overall efficiency roughly obeys the law :

$$(1 - \eta) \propto R_e^{-1/5}. \qquad \qquad \qquad \qquad \qquad \qquad \qquad \qquad (20)$$

It is believed that this rule may be applied with reasonable confidence down to Reynolds numbers of roughly 5×10^4. At lower Reynolds numbers it is anticipated that the efficiency may decrease rather more rapidly than required by equation (20).

The value of R_e recommended for this correction is the arithmetic mean of the Reynolds number of the flow through the first nozzle row and the final rotor row.

9. *Discussion of Method.*—The present method of estimating turbine performance has been described in considerable detail and the method might consequently appear to the reader as being very laborious. In practice, however, it has not been found so laborious as it might first appear. At the N.G.T.E. it has been found that to calculate the performance of a single-stage turbine about two or three manhours of work is required to set down the relevant geometric data, estimate the variation of outlet gas angle with outlet Mach number, and estimate the variation of loss coefficient with incidence on the rotor and stator rows. When this has been accomplished about six man-hours of work are required to estimate each constant-speed characteristic (as defined by about five flow quantities). A convenient tabular layout of this part of the calculation for one stage and one rotational speed is shown in Fig. 16.

Comparisons of test and calculated characteristics of a variety of single- and two-stage turbines has been made at N.G.T.E. In all the comparisons that were made the calculated efficiency in the vicinity of the turbine design operating conditions came within $\pm$ 2 per cent of the test efficiency. At a given speed and pressure ratio the calculated flow was generally within about $\pm$ 3 per cent. This infers that the working rules propounded for determining total-loss coefficients were good to within about $\pm$ 15 per cent of the true values around the design incidences and Mach numbers and the rules for determining mean gas outlet angles were good to within about $\pm$ 1 per cent and $\pm$ 1·5 per cent for gas outlet angles in the vicinity of 60 deg and 50 deg respectively.

It must be emphasised that to achieve good agreement between test and calculated flow quantities careful checking of blade throat areas is required. Small differences in blade thickness and setting angles between design values and values as manufactured and measured in an actual

---

† Reynolds number in any row is herein defined by blade chord, outlet gas velocity (relative to the row), outlet gas density, and outlet gas viscosity.

turbine can make a disproportionately large difference to blade passage throat area and hence to turbine swallowing capacity. Care should also be taken to assume the correct tip or shroud clearances since both theory and experiment have indicated that small variations in these can have a marked influence upon turbine efficiency. Finally, the working rules for assessing the loss coefficients have been derived from turbine tests in which the gas pressures and temperatures were reasonably uniform around the turbine inlet. The influence of non-uniform turbine inlet conditions on overall performance has not yet received much study but it is anticipated that non-uniformity may lead to some reduction of efficiency due to more powerful secondary flows, mixing losses, and possibly to large variations of incidence on to blade rows.

REFERENCES

No.	Author	Title, etc.
1	D. G. Ainley and G. C. R. Mathieson	An examination of the flow and pressure losses in blade rows of axial flow turbines. R. & M. 2891. 1951.
2	J. Reeman, P. Gray and C. Morris	Some Calculated Turbine Characteristics. Power Jets Report R.1111. 1945.
3	A. B. P. Beeton	A method of estimating the performance of a gas turbine stage. R.A.E. Tech. Note Eng. 330. A.R.C. 8,425. 1944.
4	D. G. Ainley	Estimation of the change in performance characteristics of a turbine resulting from changes in gas thermodynamic properties. R. & M. 2973. 1951.
5	J. Reeman and E. A. Simonis	The effect of trailing-edge thickness on blade loss. R.A.E. Tech. Note Eng. 116. 1943.
6	G. Hudson	The physical implications of representing frictional flow in convergent nozzles by a law of constant adiabatic efficiency. Power Jets Memorandum 1202. 1946.
7	S. J. E. Moyes	Note on the critical flow conditions of a gas in convergent passage and the influence of frictional losses. R.A.E. Report E.3923. 1942.

APPENDIX I

A	Gas flow area measured normal to flow direction (sq in.)
A_n	Annulus area (sq in.)
A_t	Blade passage throat area (sq in.)
c	Blade chord (in.)
C_{Dk}	Coefficient of drag on blades created by tip clearance pressure losses
C_{Ds}	Coefficient of drag on blades created by secondary flow pressure losses
C_L	Lift coefficient based on vector mean velocity
$I.D.$	Inside diameter of turbine annulus (in.)
$O.D.$	Outside diameter of turbine annulus (in.)
$M.D.$	Mid-diameter of turbine annulus (in.)

e	Mean radius of curvature of the convex surface of a blade between the throat and the trailing edge (in.) (*see* Fig. 3)
g	Acceleration due to gravity (ft/sec²)
h	Annulus height (equals blade height if radial tip clearance is zero) (in.)
i	Incidence angle of flow on to a blade row, given by difference between gas flow angle relative to blade inlet and blade inlet angle
i_s	Stalling incidence
k	Radial tip clearance or minimum shroud band clearance (in.)
K_p	Specific heat at constant pressure (ft pdl/lb/deg C.)
M	Mach number
N	Rotational speed
o	Blade opening or throat (in.)
p_s	Static pressure (lb/sq in. abs.)
P	Total pressure (lb/sq in. abs.)
Q	Non-dimensional mass flow parameter $(W\sqrt{T}/AP)$
R	Gas constant (ft pdl/lb/deg C.)
R_e	Reynolds number
s	Blade pitch or spacing (in.)
t	Maximum blade thickness (in.)
t_e	Blade trailing-edge thickness, measured normal to camber-line at trailing edge (in.)
T	Total gas temperature (deg K)
T_s	Static gas temperature (deg K)
ΔT	Gas total temperature drop across turbine (deg C.)
ΔT_{isen}	Isentropic gas total temperature drop across turbine (deg C.)
U	Rotor blade speed at reference diameter (ft/sec)
V	Gas velocity (ft/sec)
V_a	Axial component of gas velocity (ft/sec)
V_w	Whirl component of gas velocity (ft/sec)
W	Gas mass flow (lb/sec)
Y_p	Profile-loss coefficient
Y_s	Secondary-loss coefficient
Y_k	Clearance-loss coefficient
Y_t	Total-loss coefficient
α	Gas flow angle, always measured relative to the axial direction
β	Blade angle, measured relative to the axial direction
γ	Ratio of specific heats

12

Γ	V_{a2}/V_{ao}
ξ_S	Stator blade stagger angle
ξ_R	Rotor blade stagger angle
η	Isentropic total head efficiency
λ	Empirical factor defining secondary loss ($\lambda = C_{Ds}(s/c)/C_L{}^2$)
μ	Gas viscosity
ρ	Gas density
$\bar{\omega}$	Mean loss of total pressure through a blade row due to friction, flow separation, etc. (lb/sq in.)

Suffices

i	Inlet to first stator row of a turbine
o	Outlet from a stator row
1	Relative to a rotor row at inlet to the row
2	Relative to a rotor row at outlet from the row
3	Inlet to a stator row

Note : These suffices are applied to gas flow angles, blade angles, gas velocities, gas temperatures, gas pressures, gas flow areas measured normal to the flow direction, and annulus areas. At reference stations between blade rows $A_{no} = A_{n1}$ and $A_{n2} = A_{n3}$. The suffices repeat themselves from stage to stage in a turbine. The suffix 3 is also used for outlet total pressure and temperature from a multi-stage turbine, but this fact is specifically stated in text when the suffix is so used. $\alpha_{0,2}{}'$ is the estimated gas outlet angle if tip clearance were zero on a blade possessing a finite value of k.

Convention of Signs.—This has been chosen to follow directly from that already well established in axial-compressor theory in this country. The extension of the compressor system to a typical turbine stage is illustrated in Fig. 1.

It should be noted, with the arrangement drawn, that the sign of the outlet gas angles, outlet blade angles, and outlet swirl velocities *relative* to each row becomes negative for a turbine. Furthermore the blade velocity must also be regarded as negative in order that the stage temperature rise (or work done *on* the gas by the blading) shall be negative (*i.e.*, a temperature *drop* across the stage) for a turbine.

The sign to be attributed to a gas swirl velocity is always the same as that of the associated vector swirl angle.

Gas axial velocity is always positive.

It is important to appreciate that the signs to be attributed to the gas swirl angles and velocities must always be determined by reference to the blade row with which these velocity components are directly associated. In other words, the sign attributed to absolute velocities and angles (*i.e.*, velocities and angles which would be registered by instruments which are stationary relative to the machine casing) must be determined by reference to the immediately adjacent stationary blade row. The signs attributed to relative velocities and angle must be determined by reference to the immediately adjacent moving row (relative to which the velocities and angles are supposed to refer).

Note : The swirl velocity at outlet from a turbine is always *negative* when it swirls in the same direction as the direction of rotation of the rotor.

APPENDIX II

Example of a Turbine Performance Estimation

To illustrate the method of performance estimation described in the preceding report the performance of a single-stage turbine is calculated below at one speed. It is supposed that the gas temperature at turbine inlet is to be 1,100 deg K and that the speed selected is $N/\sqrt{T_i} = 435$. It will also be assumed that the inlet total pressure to the turbine is 40 lb/sq in.(absolute) at all flows. It is not essential to choose actual values for the inlet conditions ; the calculation can be carried out using non-dimensional quantities throughout. However it is considered that the calculation is easier to follow if actual quantities are used. If the final overall stage characteristics are plotted in terms of the familiar non-dimensional quantities, then the turbine performance with inlet conditions other than those selected may be easily deduced.

The geometrical dimensions of the turbine required for the calculation are set out below and an explanatory diagram is given in Fig. 13.

The required geometrical dimensions are as follows (at an inlet gas temperature of 1,100 deg K) :

Turbine Annulus Dimensions

Inner diameter of annulus (constant throughout the stage)	= 9·50 in.
Outer diameter of annulus (constant throughout the stage)	= 13·00 in.
Reference diameter	= 11·25 in.
Annulus area throughout turbine	= 61·85 sq in.

Details of Stator Row

Inlet blade angle (β_1)	= 0 deg
Blade chord (c) at reference diameter	= 1·33 in.
Blade pitch (s) ,, ,, ,,	= 0·9817 in.
Pitch/chord (s/c) at ,, ,,	= 0·739
Blade opening (o) ,, ,, ,,	= 0·429 in.
Value of e ,, ,, ,,	= 3·516 in.
s/e ,, ,, ,,	= 0·279
t/c ,, ,, ,,	= 0·200
t_e/s ,, ,, ,,	= 0·020
o/s ,, ,, ,,	= 0·437
$\cos^{-1} o/s$,, ,, ,,	= 64·1 deg
Tip clearance (k)	= 0 in.
Annulus height (h)	= 1·75 in.
Throat are (A_t)	= 26·97 sq in.
Annulus area at reference station downstream of stator row (A_{no})	= 61·85 sq in.
$\cos^{-1} (A_t/A_{no})$	= 64·1 deg

14

Details of Rotor Row

Inlet blade angle (β_1) at reference diameter				=	36·0 deg
Blade chord (c)	,,	,,	,,	=	0·95 in.
Blade pitch (s)	,,	,,	,,	=	0·7113 in.
s/c	,,	,,	,,	=	0·749
Blade opening (o)	,,	,,	,,	=	0·447 in.
e	,,	,,	,,	=	2·00 in.
s/e	,,	,,	,,	=	0·355
t/c	,,	,,	,,	=	0·15
$t_\bullet/s$	,,	,,	,,	=	0·010
o/s	,,	,,	,,	=	0·629
$\cos^{-1} o/s$	,,	,,	,,	=	51·0 deg
Tip clearance (k)				=	0·030 in.
Annulus height (h)				=	1·75 in.
k/h				=	0·01715
Throat area (A_t'), if $k = 0$ (*see* section 5.1)				=	38·9 sq in.
Annulus area at reference station downstream of rotor row				=	61·85 sq in.

Calculation of Gas Outlet Angles from the Stator Row.—When the outlet Mach number (M_o) is less than 0·5, the gas outlet angle is given by :

$$\alpha_o = \alpha_o{}^* - 4(s/e) \quad \dots \quad \dots \quad \dots \quad \dots \quad \dots \quad \text{equation (1), section 5.1}$$

$$\alpha_o{}^* = f\,(\cos^{-1} o/s) = -\,62\cdot4 \text{ deg} \quad \dots \quad \dots \quad \text{Fig. 5}$$

$$4(s/e) = 1\cdot1 :$$

therefore $\alpha_o = -\,63\cdot5$ deg.

When $M_o = 1\cdot0$:

$$\alpha_o = -\,\cos^{-1}(A_t/A_{no}) \quad \dots \quad \dots \quad \dots \quad \dots \quad \text{equation (2), section 5.1 :}$$

therefore $\alpha_o = -\,64\cdot1$ deg

Between $M_o = 0\cdot5$ and $M_o = 1\cdot0$ a smooth transition curve is sketched in as shown in Fig. 14. As stated in section 5 it is assumed that the gas outlet angle is uninfluenced by the gas incidence angle on to the blade row.

Calculation of Gas Outlet Angles for the Rotor Row.—When $M_2 < 0\cdot5$ the outlet gas angle is first estimated from equation (1), section 5.1, and is then corrected for the finite blade tip clearance by use of equation (4).

Thus, with zero clearance,

$$\alpha_2 = \alpha_2{}^* - 4(s/e) \qquad\qquad\qquad\qquad\qquad\qquad\qquad \text{equation (1)}$$

$$\alpha_2{}^* = f\,(\cos^{-1} o/s) = -\,47\cdot2 \text{ deg} \qquad\qquad\qquad\qquad\qquad\qquad \text{Fig. (5)}$$

$$4(s/e) = 1\cdot4 :$$

therefore $\qquad \alpha_2 = -\,48\cdot6$ deg.

Correcting for tip clearance, using equation (4) :

$$\alpha_2 = \tan^{-1}\{[1 - X(k/h)(\cos \beta_1/\cos \alpha_2{}')]\,\tan \alpha_2{}' + X(k/h)(\cos \beta_1/\cos \alpha_2{}')\,\tan \beta_1\}$$

and $X = 1\cdot35$ for radial tip clearance,

also $\qquad k/h = 0\cdot01715 :$

therefore $\qquad \alpha_2 = \tan^{-1}\{(1 - 0\cdot0284)(-\,1\cdot134) + 0\cdot0284 \times 0\cdot726\} :$

therefore $\qquad \underline{\alpha_2 = -\,47\cdot3 \text{ deg.}}$

When $M_2 = 1\cdot0$ the outlet gas angle is given by equation (2), *viz.*,

$$\alpha_2 = -\,\cos^{-1}(A_t/A_{n\,2}).$$

If the tip clearance were zero the throat area of the blade $(A_t{}')$ would be $38\cdot9$ sq in. With a tip clearance (k) of $0\cdot030$ in. the throat area of the blade is

$$A_t = A_t{}'\,[1 - (k/h)] + \pi \times k \times O.D.$$

$$= 38\cdot9\,[1 - 0\cdot01715] + \pi \times 0\cdot030 \times 13 = 39\cdot46 \text{ sq in.}$$

Therefore when $M_2 = 1\cdot0$

$$\alpha_2 = -\,\cos^{-1}(39\cdot46/61\cdot85) :$$

therefore $\qquad \alpha_2 = -\,50\cdot3$ deg.

Between $M_2 = 0\cdot5$ and $M_2 = 1\cdot0$ a smooth transition curve is sketched in as shown in **Fig. 14.**

Calculation of Stator-Loss Coefficient.—Since the stator row operates at one incidence only $(i = 0 \text{ deg})$ it is only necessary to predict the loss coefficient for this one incidence.

(*a*) *Profile Loss*

$$\beta_i = 0 \text{ deg}, \;\; \alpha_0 = -\,63\cdot5 \text{ deg}, \;\; s/c = 0\cdot739, \;\; \beta_i/\alpha_o = 0, \;\; t/c = 0\cdot20.$$

From Fig. 4 and equation (5) $\underline{Y_p = 0\cdot0288}$

(*b*) *Secondary and Tip Clearance Loss.*—At zero incidence : $\alpha_i = 0$, $\alpha_o = -\,63\cdot5$ deg, $s/c = 0\cdot739$, $k/h = 0$

Now, $\qquad C_L/(s/c) = 2(\tan \alpha_i - \tan \alpha_o)\cos \alpha_m$

where $\qquad \tan \alpha_m = (1/2)\,(\tan \alpha_i + \tan \alpha_o)$

therefore $C_L/(s/c) = 2\cdot83$, and $\cos^2 \alpha_o/\cos^3 \alpha_m = 0\cdot566$

The expression for secondary and clearance loss is given by question (6) :

$$Y_s + Y_k = [\lambda + B(k/h)][C_L/(s/c)]^2\,[\cos^2 \alpha_o/\cos^3 \alpha_m]$$

The factor λ is a function of $(A_0/A_i)^2/[1 + I.D./O.D.]$ and is plotted in Fig. 8.

16

$$A_i = A_{n\,i} \cos \beta_i = A_n = 61 \cdot 85 \text{ sq in.}$$

$$A_0 = A_{n\,0} \cos \alpha_0 = 27 \cdot 60 \text{ sq in.}$$

$$I.D./O.D. = 9 \cdot 5/13 \cdot 0 = 0 \cdot 73$$

therefore $\qquad (A_0/A_i)^2/(1 + I.D./I.D.) = 0 \cdot 115$

therefore $\qquad \lambda = 0 \cdot 0065$ $\qquad$ .. $\qquad$ .. $\qquad$ .. $\qquad$ .. $\qquad$ .. $\qquad$ .. $\qquad$ .. $\qquad$ .. Fig. 8

therefore $Y_s + Y_k = 0 \cdot 0065 \times (2 \cdot 83)^2 \times 0 \cdot 566 = 0 \cdot 0295$

Total Loss Coefficient

$$Y_t = Y_p + Y_s + Y_k = 0 \cdot 0288 + 0 \cdot 0295$$

therefore $\qquad \underline{Y_t = 0 \cdot 0583}$

Since $t_e/s = 0 \cdot 02$ no correction is required for trailing-edge thickness. This total-loss coefficient, calculated from predicted gas angles for $M_o < 0 \cdot 5$, is assumed to remain constant at all values of M_o.

Calculation of Rotor Row Loss Coefficients.—Profile Loss.—Relevant data for determining profile-loss coefficient at zero incidence is :

$$\beta_1 = 36 \cdot 0 \text{ deg} ; \quad \alpha_2 = -48 \cdot 6 \text{ deg} \quad \text{(Note that value of } \alpha_2 \text{ for zero clearance is used for predicting loss coefficient).}$$

$$s/c = 0 \cdot 749 ; \quad \beta_1/\alpha_2 = -0 \cdot 74 ; \quad t/c = 0 \cdot 15$$

$$\left. \begin{array}{l} Y_p(\beta_1 = 0 \text{ deg}) = 0 \cdot 00238 \\ \\ Y_p(\beta_1 = -\alpha_2) = 0 \cdot 0722 \end{array} \right\} \text{ Fig. 4.}$$

Profile loss at zero incidence is given by equation (5) :

$$Y_p = \{Y_p(\beta_1 = 0 \text{ deg}) + (\beta_1/\alpha_2)^2 \, [Y_p(\beta_1 = -\alpha_2) - Y_p(\beta_1 = 0 \text{ deg})]\} \left[\frac{t/c}{0 \cdot 2}\right]^{-\beta_1/\alpha_2}$$

$$= \{0 \cdot 0238 + (-0 \cdot 74)^2 \, (0 \cdot 0484)\} \, [0 \cdot 75]^{0 \cdot 74}$$

$$= 0 \cdot 0503 \times 0 \cdot 808 = 0 \cdot 0406.$$

To calculate the profile-loss coefficient at incidences other than zero it is necessary to evaluate the stalling incidence, i_s, and employ the relationship of $Y_p/Y_p(i = 0)$ with i/i_s plotted in Fig. 6.

The stalling incidence is evaluated as described in section 5.2. Thus :

$$\beta_1 = 36 \cdot 0 \text{ deg}, \quad \alpha_2 = -48 \cdot 6 \text{ deg}, \quad s/c = 0 \cdot 749.$$

As the pitch/chord ratio is virtually $0 \cdot 75$ the curves of Fig. 7b can be used directly

$$\beta_1/\alpha_2(s/c = 0 \cdot 75) = -0 \cdot 74$$

therefore $\qquad i_s = 9 \cdot 5 \text{ deg.}$ $\qquad$ .. $\qquad$ .. $\qquad$ .. $\qquad$ .. $\qquad$ .. $\qquad$ .. $\qquad$ .. $\qquad$ .. Fig. 7b

Secondary and Clearance Loss.—From equation (6) :

$$Y_s + Y_k = [\lambda + B(k/h)][C_L/(s/c)]^2[\cos^2 \alpha_2/\cos^3 \alpha_m].$$

For the rotor row, $A_1 = A_{n\,o} \cos \beta_1 = 50 \cdot 0 \text{ sq in.}$

and $A_2 = A_{n\,2} \cos \alpha_2 = 40 \cdot 9 \text{ sq in.}$

Therefore $(A_2/A_1)^2/(1 + I.D./O.D.) = 0 \cdot 386$

and from Fig. 8, $\qquad \lambda = 0 \cdot 0183.$

Furthermore $B = 0\cdot50$ for radial clearance and $k/h = 0\cdot01715$.

Therefore $Y_s + Y_k = 0\cdot0269[C_L/(s/c)]^2[\cos^2\alpha_2/\cos^3\alpha_m]$.

This equation must be evaluated for a number of incidence angles. This may best be done in tabular form as shown in the following table together with the profile loss and final evaluation of total-loss coefficient.

Total-Loss Coefficient

i/i_s	$-3\cdot0$	$-1\cdot5$	$-0\cdot8$	0	$1\cdot0$	$1\cdot5$
i	$-28\cdot5$	$-14\cdot3$	$-7\cdot6$	0	$9\cdot5$	$14\cdot3$
α_1	$+7\cdot5$	$+21\cdot7$	$+28\cdot4$	$+36$	$+45\cdot5$	$+50\cdot3$
$C_L/(s/c)$	—	$2\cdot88$	$3\cdot22$	$3\cdot65$	$4\cdot30$	—
$\cos^2\alpha_2/\cos^3\alpha_m$	—	$0\cdot528$	$0\cdot494$	$0\cdot465$	$0\cdot44$	—
$Y_s + Y_k$	$0\cdot1178$	$0\cdot1178$	$0\cdot1378$	$0\cdot1668$	$0\cdot2186$	$0\cdot2186$
Y_p	$0\cdot1739$	$0\cdot0853$	$0\cdot0565$	$0\cdot0406$	$0\cdot0812$	$0\cdot1820$
Y_t	$0\cdot2917$	$0\cdot2031$	$0\cdot1943$	$0\cdot2074$	$0\cdot2998$	$0\cdot4006$

These values of Y_t correspond to $t_e/s = 0\cdot02$. Since on this rotor $t_e/s = 0\cdot01$ the total-loss coefficients as calculated above must be corrected for trailing-edge thickness. This is achieved by multiplying the loss coefficients by an appropriate factor obtained from Fig. 9. For $t_e/s = 0\cdot01$ this factor is $0\cdot96$. We have a final estimated variation of total-loss coefficient with incidence therefore as below :

i (deg)	$-28\cdot5$	$-14\cdot3$	$-7\cdot6$	0	$9\cdot5$	$14\cdot3$
Y_t	$0\cdot2800$	$0\cdot1950$	$0\cdot1867$	$0\cdot199$	$0\cdot288$	$0\cdot3845$

These values are plotted in Fig. 14.

Calculation of the Turbine Characteristic.—Having determined the loss coefficients and gas outlet angles for the individual rows it is possible to commence the step-by-step calculation of the gas flow conditions at entry to and exit from each row for selected entry conditions and rotational speed.

For demonstration the following entry conditions are arbitrarily selected for the turbine :

$P_i = 40$ lb/sq in., absolute

$T_i = 1100$ deg K

$N/\sqrt{T_i} = 435$.

These conditions represent a blade speed at the reference diameter ($11\cdot25$ in.) of -708 ft per sec, the negative sign being inserted in accordance with the chosen sign convention. The 'standard' thermodynamic gas constants used throughout are :

$K_p = 12{,}300$ ft pdl/lb/deg C.

$R = 3{,}073$ ft pdl/lb/deg C.

$\gamma = 1\cdot3330$.

It is now necessary to select arbitrarily a number of mass flows through the turbine. For each mass flow the inlet and outlet conditions for each blade row are estimated in the manner described in sections 6 to 6.4. The calculation can conveniently be carried out in a tabular form, gas conditions for several mass flow values being calculated concurrently. A table of calculation for the present turbine is set out in full on Fig. 16 with an explanatory note attached to each step.

In this example the first five selected flows are found to pass through the stage without the outlet Mach numbers from either the nozzle or the rotor row exceeding the critical Mach number, *i.e.*, the non-dimensional flows through each row are less than the maximum flow that can be passed by the row. The sixth selected flow is exactly equal to the maximum flow that can be passed by the nozzle row but it is found that in this instance the non-dimensional flow relative to the rotor row (*see* line 32) is greater than the maximum possible values (line 34) that can be passed by the rotor. This latter flow is therefore an impossible value and the calculation of the flow conditions with this initial mass flow must be discontinued. When this impasse is encountered it becomes necessary to select an initial flow which will just pass through the rotor row. This flow can be selected by a process of interpolation by plotting both the non-dimensional flow through the rotor (line 32) and the maximum possible non-dimensional flow (line 34) against the initial flow (W or $W\sqrt{T_i}/P_i$). The point at which these two curves intersect then represents the maximum flow which the turbine will pass. In the present case this flow is given by $W\sqrt{T_i}/P_i = 10\cdot268$ and the calculation for this flow is carried through in the seventh column of the table in Fig. 16. At this flow the relative outlet Mach number from the rotor is exactly equal to the critical value for the relevant rotor loss coefficient. In accordance with the assumptions outlined in section 7 it is now supposed that if the total pressure drop across the turbine exceeds the critical drop calculated in column 7 then (*a*) further increase in pressure drop across the turbine is not accompanied by any further increase in flow, (*b*) the flow conditions upstream of the rotor remain fixed (*i.e.*, identical to the values calculated in column 7 down to line 30) and (*c*) further gas expansion takes place only downstream of the rotor row with the rotor loss coefficient remaining unaltered and the relative gas outlet angle adjusting itself just sufficiently to maintain continuity of flow.

To demonstrate the altered procedure after the flow has attained its maximum value columns eight and nine are added on Fig. 16. Values of M_2 at the rotor outlet (line 42) are now arbitrarily selected. Uniquely related with these Mach numbers are the non-dimensional flow parameter at rotor outlet, $W\sqrt{T_2}/A_2P_2$ (*see* table in Appendix IV), and the total to static-pressure ratio p_{s2}/P_2. Also known is the rotor loss coefficient and the inlet total pressure, P_1, and outlet total temperature T_2 (equal to T_1). These conditions are sufficient to determine the gas outlet angle α_2, required to preserve continuity of flow. Thus :

$$\bar{\omega}/P_2 = Y_i[1 - p_{s2}/P_2] \quad \ldots \qquad \ldots \qquad \ldots \qquad \ldots \qquad \ldots \qquad \ldots \qquad \ldots \qquad \ldots \qquad (21)$$

$$\bar{\omega}/P_1 = (\bar{\omega}/P_2)/(1 + \bar{\omega}/P_2) \qquad \ldots \qquad \ldots \qquad \ldots \qquad \ldots \qquad \ldots \qquad \ldots \qquad \ldots \qquad (22)$$

$$P_2 = P_1 - \bar{\omega}. \qquad \ldots \qquad \ldots \qquad \ldots \qquad \ldots \qquad \ldots \qquad \ldots \qquad \ldots \qquad \ldots \qquad (23)$$

From value of $W\sqrt{T_2}/A_2P_2$ in line 49 and the known values of W, T_2, and P_2 we can find the necessary value of A_2. Since $A_2 = A_{n2} \cos \alpha_2$ we can determine α_2 (line 51). Having thus determined the new outlet conditions relative to the rotor the absolute conditions at the rotor outlet can be calculated as before (lines 52 to 64).

From the initial and final pressures and temperatures the overall stage values of pressure ratios, efficiency, etc., are calculated in lines 65 to 70 and plotted in Fig. 15.

These characteristics correspond to a mean blade Reynolds number of 2×10^5. The overall efficiency and temperature ratio may be roughly corrected to other Reynolds numbers by use of equation (20), section 7.

In this particular example the flow was limited or choked by the rotor row. This is not, of course, peculiar to all turbines. If the nozzle row is found to choke first then when the performance at pressure ratios beyond the critical are calculated the same procedure that has been outlined for the choked rotor must be applied to the nozzle. In such an instance, of course, the tabular layout shown in Fig. 16 would have to be modified accordingly. Generally it may be found more convenient to continue the calculation of the performance of the turbine under choked conditions on a second table rather than to concentrate the entire performance into one table as shown here.

APPENDIX III

Interpolation of Constant-speed Characteristics

If the characteristics of a turbine are required for a large number of speeds it is only necessary in general to perform the detailed calculations as set out in the preceding sections for two speeds— preferably a speed close to the highest speed and a speed close to the lowest speed of the required range.

If the gas was nearly incompressible then the turbine performance at various speeds could be roughly related on a pair of curves by plotting efficiency and $(W\sqrt{T_i}/P_i)/(N/\sqrt{T_i})$ against $(K_p\Delta T/T_i)/(N/\sqrt{T_i})^2$ since $(W\sqrt{T_i}/P_i)/(N/\sqrt{T_i})$ would be proportional to the familiar velocity coefficient V_a/U and $(K_p\Delta T/T_i)/(N/\sqrt{T_i})^2$ is proportional to the familiar temperature drop coefficient $2K_p\Delta T/U^2$.

This principle can be extended to compressible gases with some degree of success if the ratio of non-dimensional inlet flow to non-dimensional speed $(W\sqrt{T_i}/P_i)/(N/\sqrt{T_i})$, is multiplied by a suitable function of the overall density ratio. On single and two-stage turbines operating with pressure ratios up to about $0\cdot3$ it has been found that plotting $(W\sqrt{T_i}/P_i)(P_iT_3/P_3T_i)^n/(N/\sqrt{T_i})$ and efficiency against $(K_p\Delta T/T_i)/(N/\sqrt{T_i})^2$ brings constant-speed characteristics at different speeds sufficiently close together to permit reasonably accurate interpolation (*N.B.* in the preceding expressions P_3 and T_3 are supposed to be the outlet total pressure and temperature from a turbine). It will be noted that the expression (P_iT_3/P_3T_i) is the overall density ratio of the gas and the power factor n is entirely empirical.

The value of n is selected by trial error to bring the curves of $(W\sqrt{T_i}/P_i)(P_iT_3/P_3T_i)^n/(N/\sqrt{T_i})$ plotted against $(K_p\Delta T/T_i)/(N/\sqrt{T_i})^2$ for the two calculated rotational speeds as close together as possible. The best value for n generally lies in the range $0\cdot5 < n < 1\cdot0$.
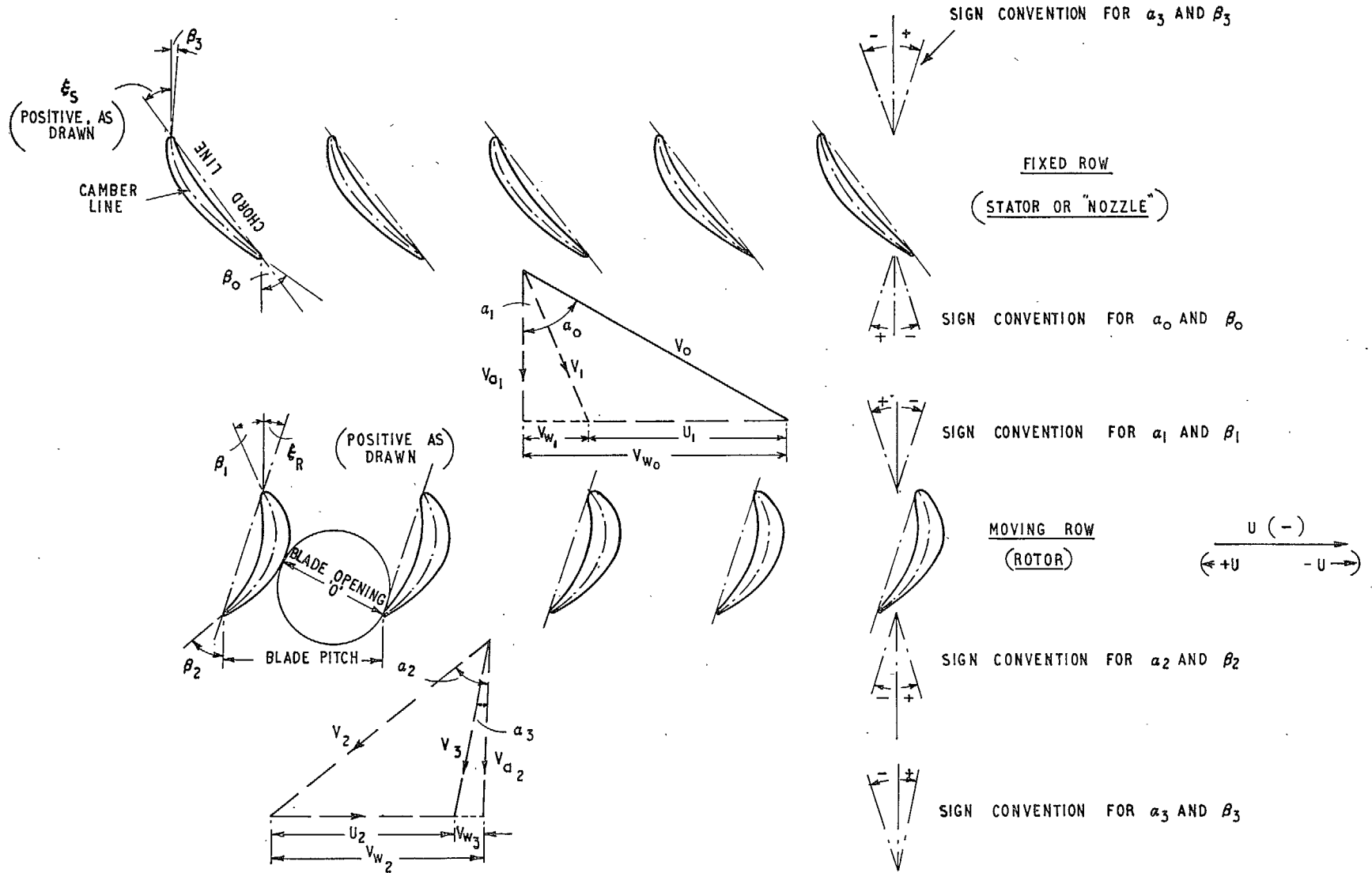
APPENDIX IV

Relationship Between Non-dimensional Flow
Parameters $W\sqrt{T}/AP$, p_s/P, M and $V/\sqrt{T}$
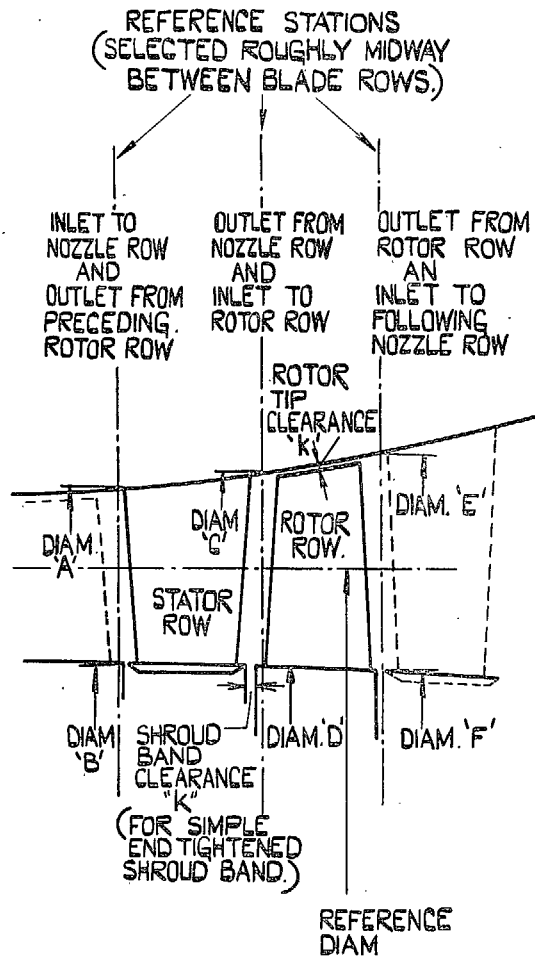
All values tabulated have been calculated for :

$\gamma = 1\cdot3330$
$K_p = 12,300$ ft pdls/lb/deg C.
$R = 3,073$ ft pdls/lb/deg C.
$g = 32\cdot173$ ft/sec^2

M	$W\sqrt{T}/AP$	p_s/P	$V/\sqrt{T}$	M	$W\sqrt{T}/AP$	p_s/P	$V/\sqrt{T}$
0·02	0·0135	0·99973	1·290	0·62	0·3342	0·7802	38·45
0·04	0·0268	0·99893	2·565	0·64	0·3404	0·7678	39·64
0·06	0·04016	0·9976	3·845	0·66	0·346	0·7555	40·80
0·08	0·05345	0·99574	5·135	0·68	0·3515	0·7427	41·99
0·10	0·06667	0·99335	6·400	0·70	0·35625	0·7307	43·06
0·12	0·0798	0·9904	7·678	0·72	0·361	0·718	44·20
0·14	0·09278	0·9870	8·95	0·74	0·3653	0·7052	45·35
0·16	0·1055	0·98317	10·21	0·76	0·3694	0·6914	46·49
0·18	0·1184	0·9787	11·495	0·78	0·3729	0·6791	47·60
0·20	0·1309	0·9738	12·75	0·80	0·3761	0·6665	48·70
0·22	0·1433	0·96835	14·024	0·82	0·37875	0·655	49·71
0·24	0·1554	0·9626	15·25	0·84	0·3814	0·6408	50·9
0·26	0·1673	0·9563	16·52	0·86	0·3837	0·6276	52·01
0·28	0·17925	0·9495	17·80	0·88	0·3856	0·6141	53·14
0·30	0·1909	0·942	19·09	0·90	0·3872	0·6025	54·20
0·32	0·20225	0·9344	20·32	0·92	0·3885	0·589	55·20
0·34	0·2131	0·9265	21·53	0·94	0·3895	0·5755	56·39
0·36	0·2238	0·9180	22·80	0·96	0·3901	0·565	57·30
0·38	0·2343	0·9092	24·02	0·98	0·3905	0·551	58·25
0·40	0·2442	0·9003	25·25	1·00	0·3907	0·540	59·25
0·42	0·2543	0·8908	26·5	1·02	0·3905	0·528	60·35
0·44	0·26375	0·8810	27·68	1·04	0·3901	0·517	61·30
0·46	0·273	0·8706	28·9	1·06	0·3895	0·504	62·2
0·48	0·2819	0·860	30·12	1·08	0·3886	0·491	63·29
0·50	0·2903	0·8495	31·31	1·10	0·3875	0·480	64·20
0·52	0·2986	0·8386	32·57	1·12	0·3861	0·4682	65·20
0·54	0·3064	0·8272	33·76	1·14	0·3846	0·4565	66·20
0·56	0·3139	0·8157	34·95	1·16	0·3828	0·4453	67·12
0·58	0·321	0·804	36·16	1·18	0·3807	0·4333	68·08
0·60	0·3278	0·7922	37·31	1·20	0·3786	0·4225	68·95

B

SIGN CONVENTION FOR α_3 AND β_3

FIXED ROW

(STATOR OR "NOZZLE")

SIGN CONVENTION FOR α_0 AND β_0

SIGN CONVENTION FOR α_1 AND β_1

MOVING ROW

(ROTOR)

$U\ (-)$

SIGN CONVENTION FOR α_2 AND β_2

SIGN CONVENTION FOR α_3 AND β_3

NOTE :- WHEN THE STAGGER ANGLE IS POSITIVE IN SIGN THEN THE ANGLE DEFINED BY $\cos^{-1} o/s$ MUST BE ASSIGNED NEGATIVE

FIG. 1. Notation and sign convention for velocity triangles on an axial-flow turbine stage. (Positive stagger on blades).

REFERENCE STATIONS
(SELECTED ROUGHLY MIDWAY
BETWEEN BLADE ROWS)

INLET TO
NOZZLE ROW
AND
OUTLET FROM
PRECEDING
ROTOR ROW

OUTLET FROM
NOZZLE ROW
AND
INLET TO
ROTOR ROW

OUTLET FROM
ROTOR ROW
AN
INLET TO
FOLLOWING
NOZZLE ROW

ROTOR
TIP
CLEARANCE
"k"

DIAM. 'E'

DIAM
'A'

DIAM
'C'

ROTOR
ROW.

STATOR
ROW

DIAM
'B'

SHROUD
BAND
CLEARANCE
"K"
(FOR SIMPLE
END TIGHTENED
SHROUD BAND.)

DIAM.'D'

DIAM. 'F'

REFERENCE
DIAM

REFERENCE DIAM. = $(A + B + 2C + 2D + E + F)/8$.

FIG. 2. Typical turbine stage showing choice of reference stations
and reference diameter for calculations.

SIGN CONVENTION FOR β_1

CAMBER LINE

SIGN CONVENTION FOR β_2
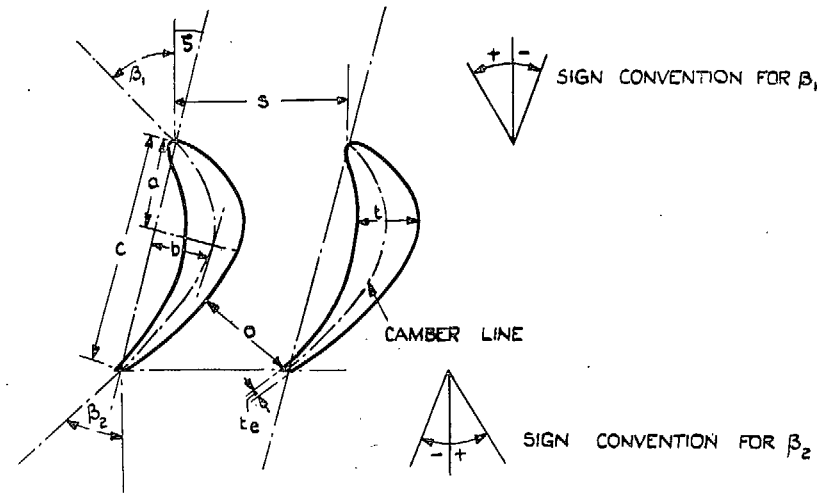
a = DISTANCE OF POINT OF MAX CAMBER FROM L.E.
b = MAXIMUM CAMBER
c = CHORD
e = MEAN RADIUS OF CURVATURE OF UPPER
    BLADE SURFACE BETWEEN THROAT AND T.E.
o = BLADE "OPENING" OR "THROAT"

s = BLADE PITCH
t = MAX THICKNESS
t_e= T.E THICKNESS
β_1= INLET BLADE ANGLE
β_2= OUTLET BLADE ANGLE
ξ= STAGGER ANGLE

TRAILING
EDGE
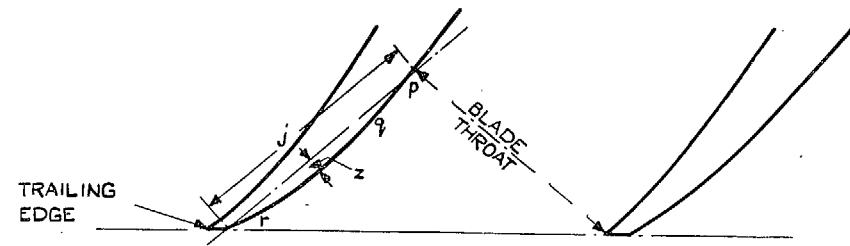
BLADE
THROAT
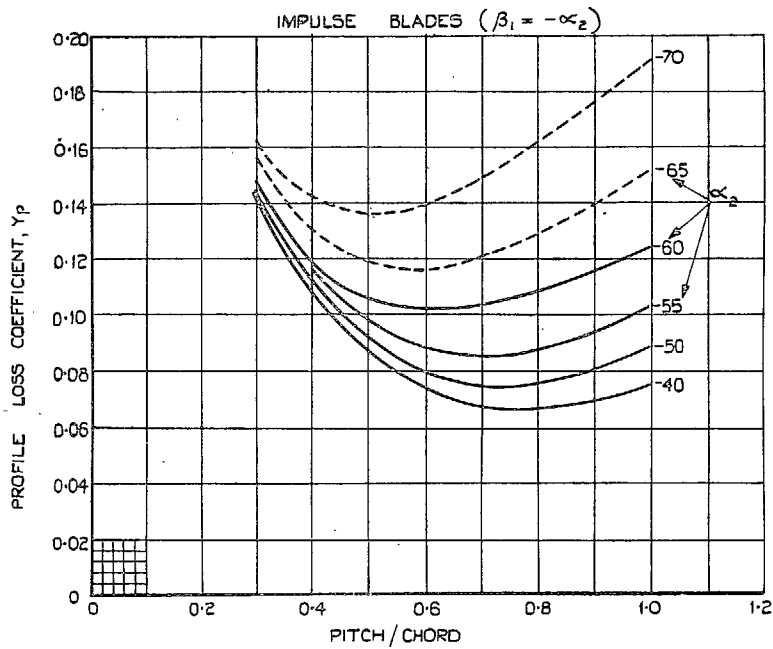
MEAN RADIUS OF CURVATURE OF $pqr = e = j^2/8z$

DETAIL OF TRAILING EDGE ILLUSTRATING CURVATURE
OF UPPER (CONVEX) SURFACE BETWEEN BLADE
THROAT AND TRAILING EDGE.

FIG. 3. Turbine blade nomenclature.

NOZZLE BLADES ($\beta_l = 0$)

VALUES OF
OUTLET GAS ANGLE α_2

(a)

IMPULSE BLADES ($\beta_l = -\alpha_2$)
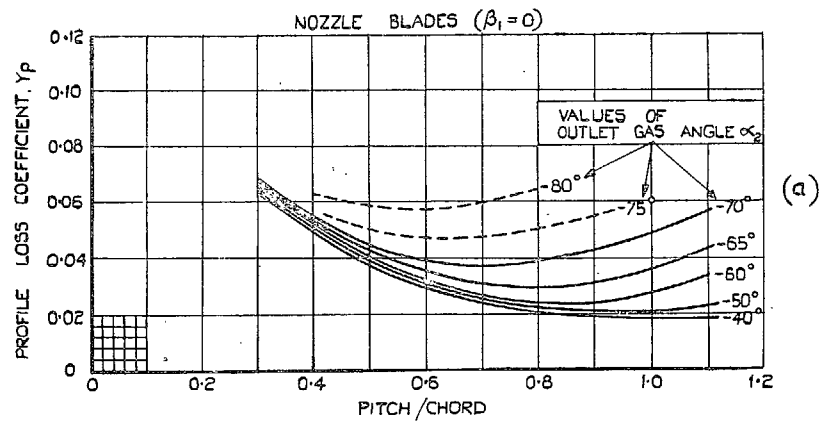
(b)

FIG. 4. Profile-loss coefficients for conventional section blades at zero incidence. ($t/c = 20$ per cent ; $R_e = 2 \times 10^5$; $M < 0.6$.)
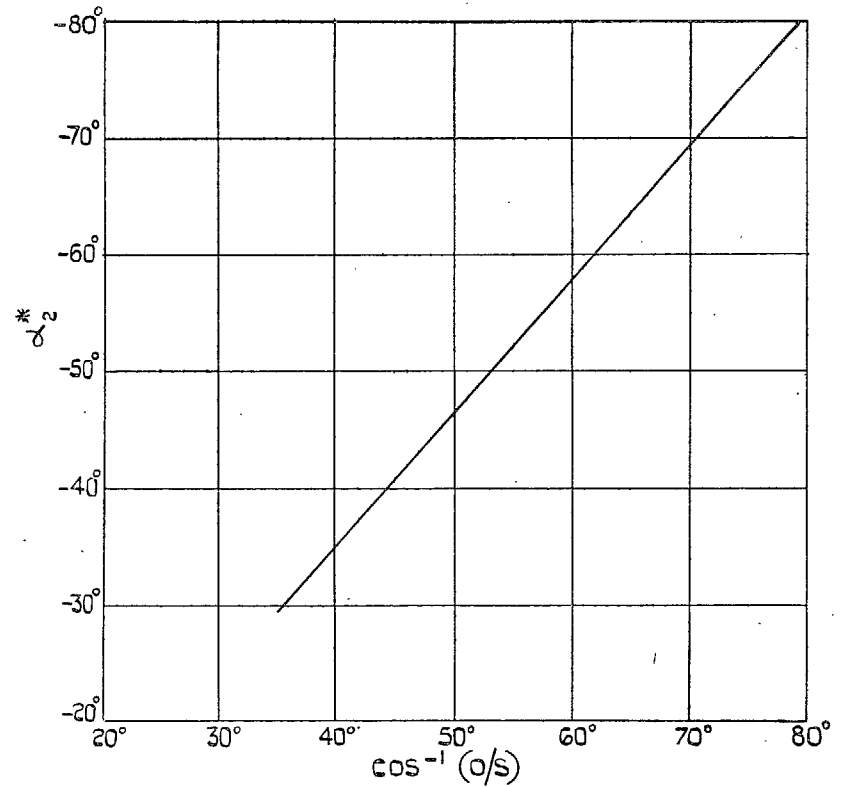
FIG. 5. Relationship between gas outlet angles and $\cos^{-1}(o/s)$ for 'straight-backed' blades operating at low Mach numbers. $M_2 < 0.5$, $R_e \simeq 2 \times 10^5$.
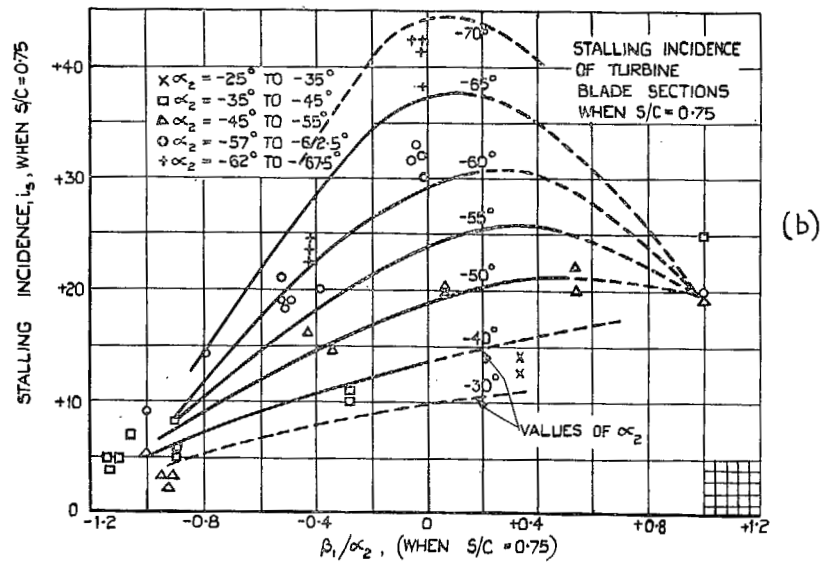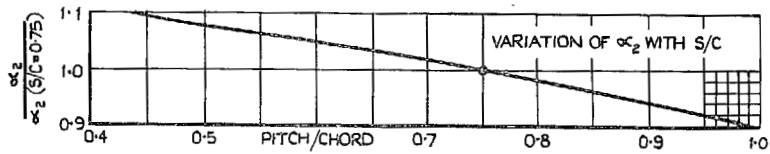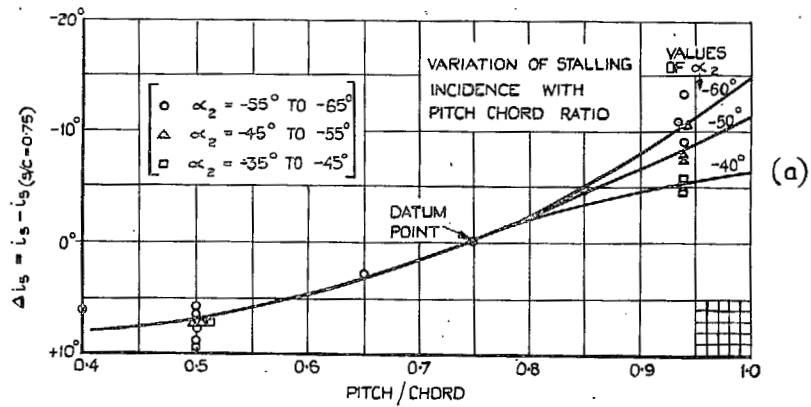
VARIATION OF STALLING INCIDENCE WITH PITCH CHORD RATIO

$\alpha_2 = -55°$ TO $-65°$
$\alpha_2 = -45°$ TO $-55°$
$\alpha_2 = -35°$ TO $-45°$

DATUM POINT

(a)

$\Delta i_s = i_s - i_{s\,(s/c=0.75)}$

PITCH / CHORD

VALUES OF α_2
$-60°$
$-50°$
$-40°$

VARIATION OF α_2 WITH S/C

$\dfrac{\alpha_2}{\alpha_2\,(S/C=0.75)}$

PITCH/CHORD

25

STALLING INCIDENCE OF TURBINE BLADE SECTIONS WHEN S/C = 0.75

$\times \alpha_2 = -25°$ TO $-35°$
$\square \alpha_2 = -35°$ TO $-45°$
$\triangle \alpha_2 = -45°$ TO $-55°$
$\bigcirc \alpha_2 = -57°$ TO $-62.5°$
$+ \alpha_2 = -62°$ TO $-67.5°$

STALLING   INCIDENCE, i_s, WHEN S/C = 0.75

$-70°$
$-65°$
$-60°$
$-55°$
$-50°$
$-40°$
$-30°$
VALUES OF α_2

(b)

β_1/α_2 , (WHEN S/C = 0.75)

FIG. 7.   Positive stalling incidences of cascades of turbine blades.
$(R_e = 2 \times 10^5 \,; M < 0.6.)$
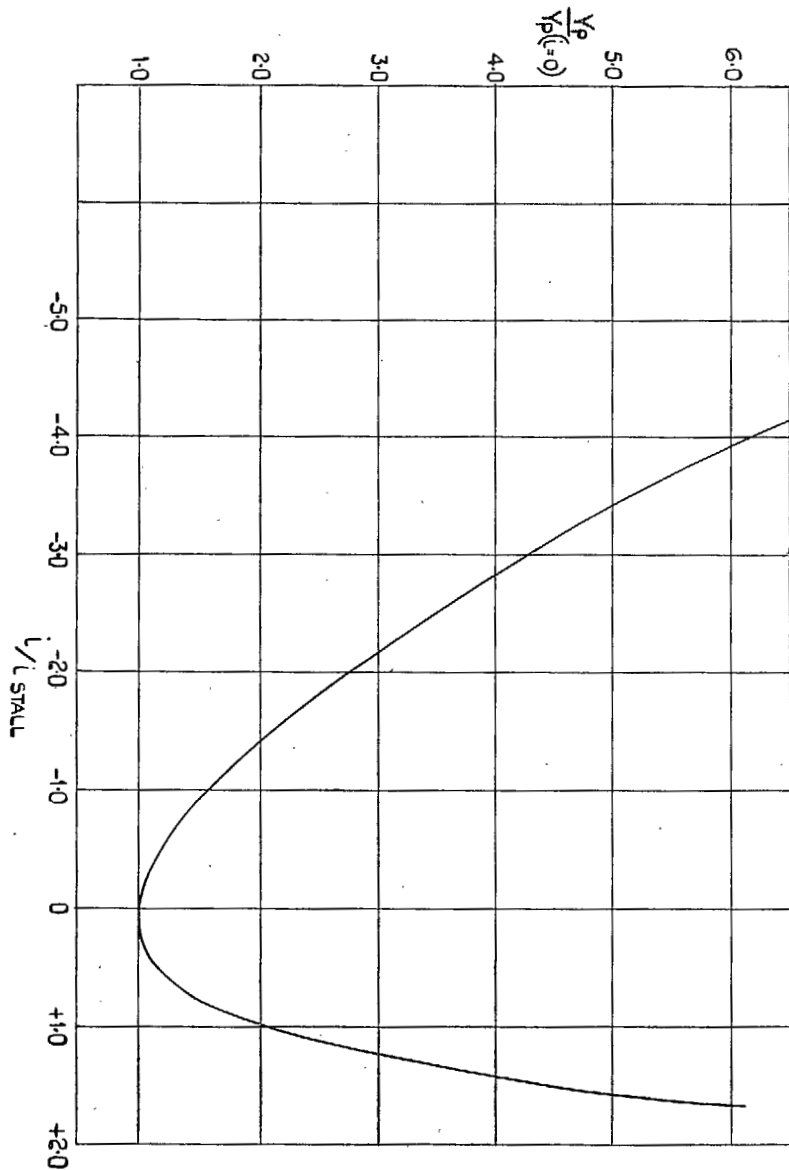
$\dfrac{Y_P}{Y_{P\,(i=0)}}$

i / i STALL

FIG. 6.   Variation of profile loss with incidence for typical turbine blading.
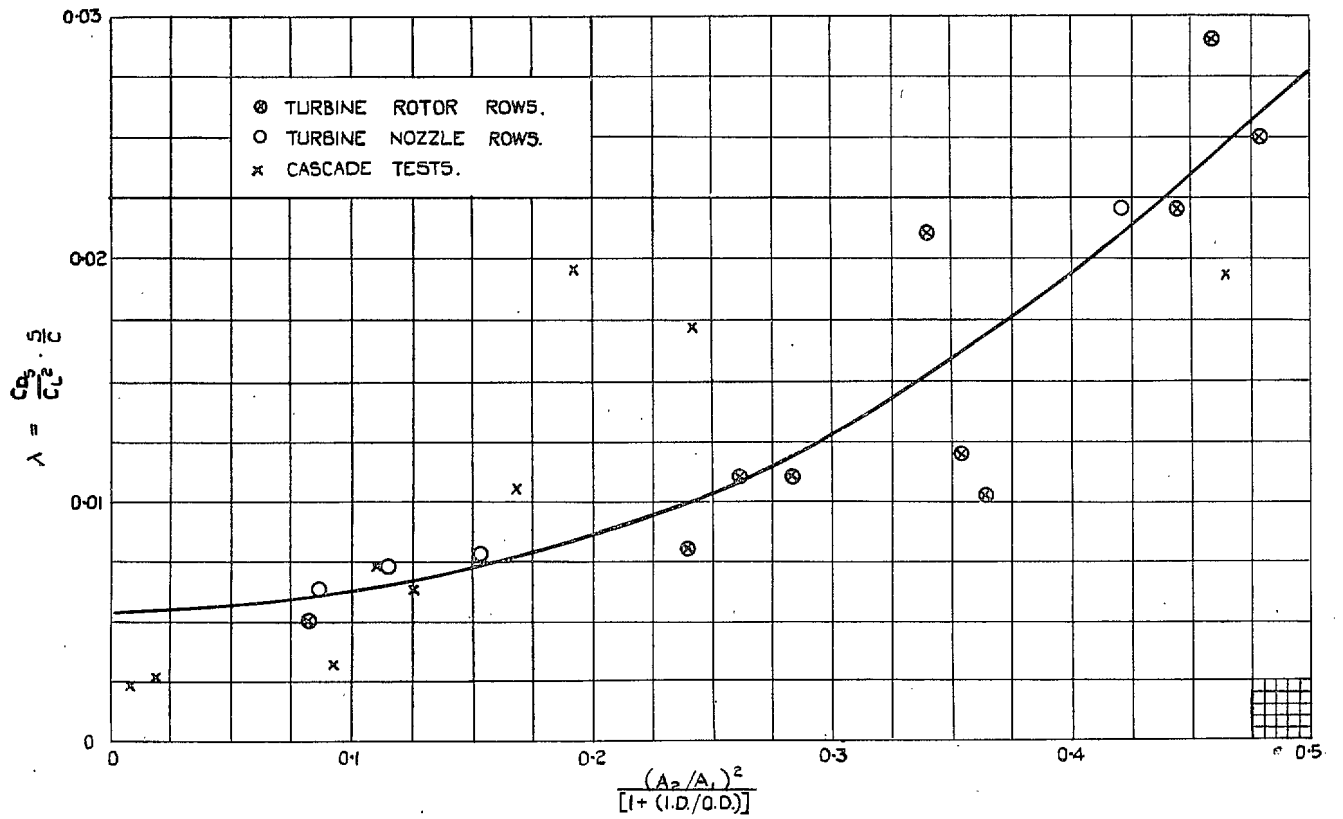
FIG. 8. Secondary losses in turbine blade rows.
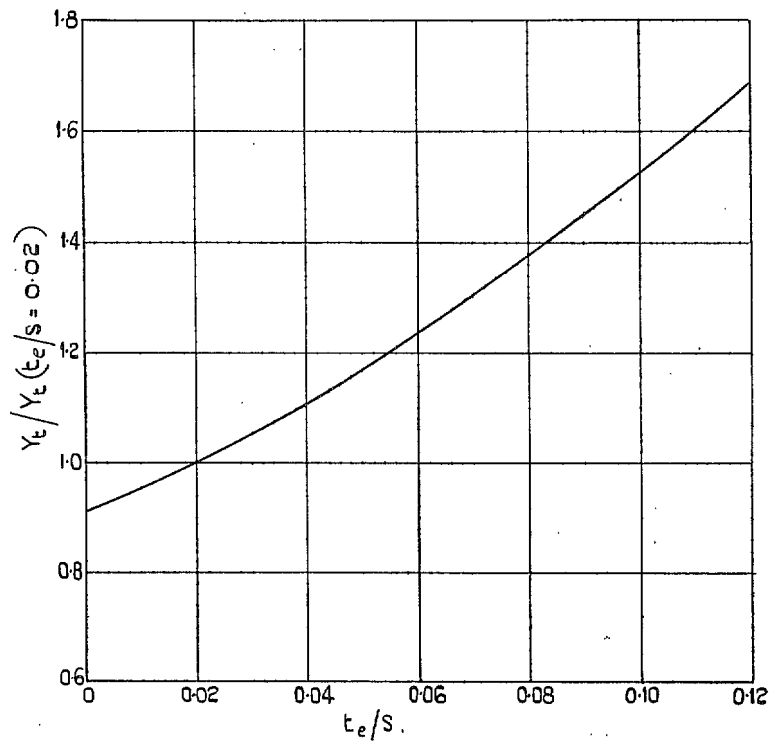

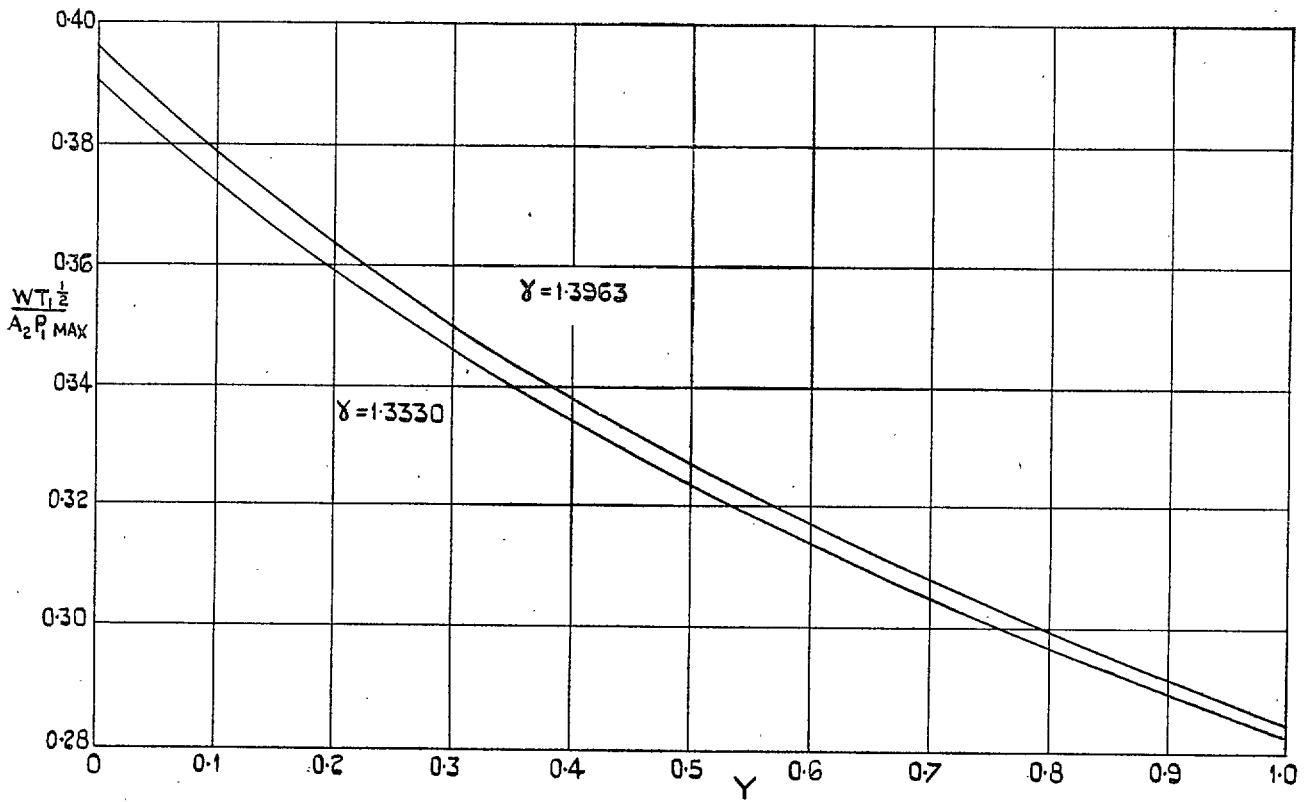FIG. 9. Effect of trailing-edge thickness on blade loss coefficients.

26

FIG. 10.   Compressible adiabatic flow.
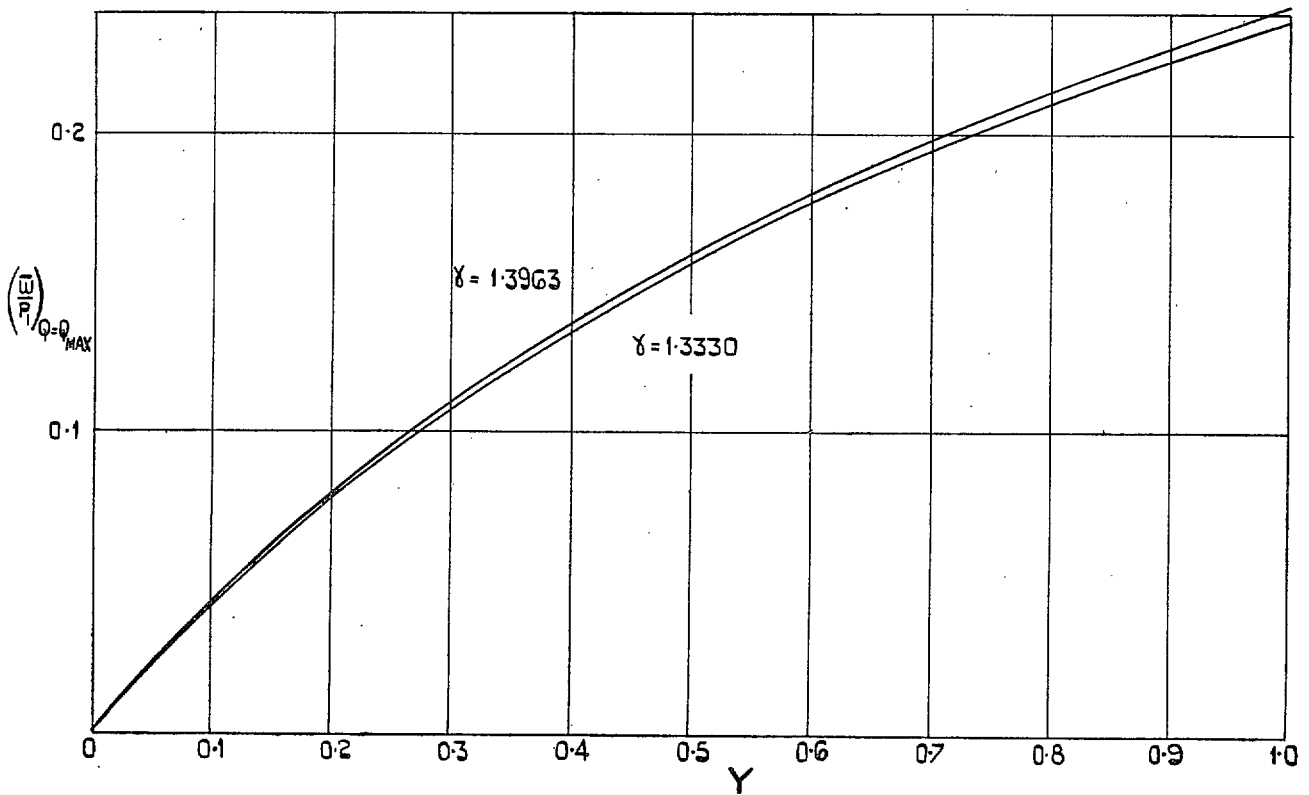

FIG. 11.   Compressible adiabatic flow.

27
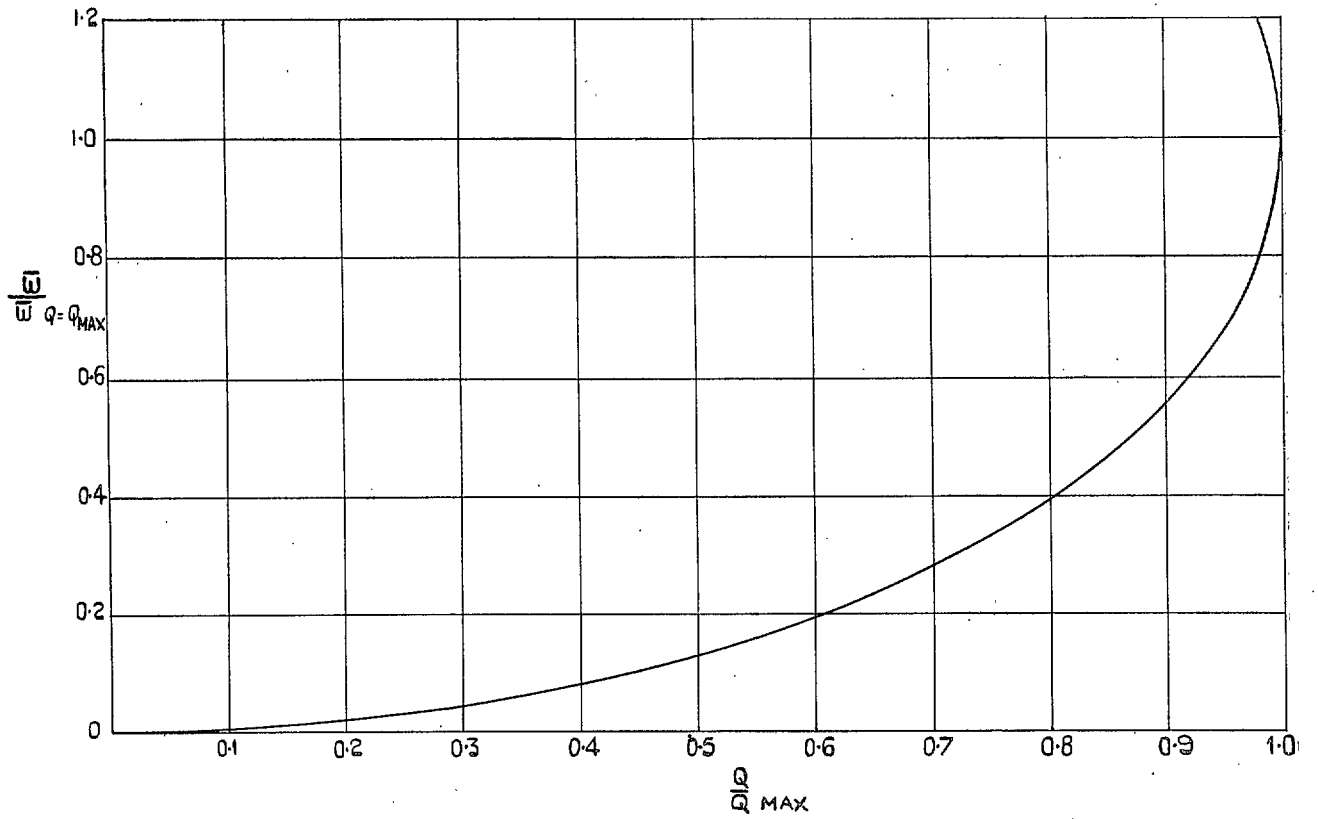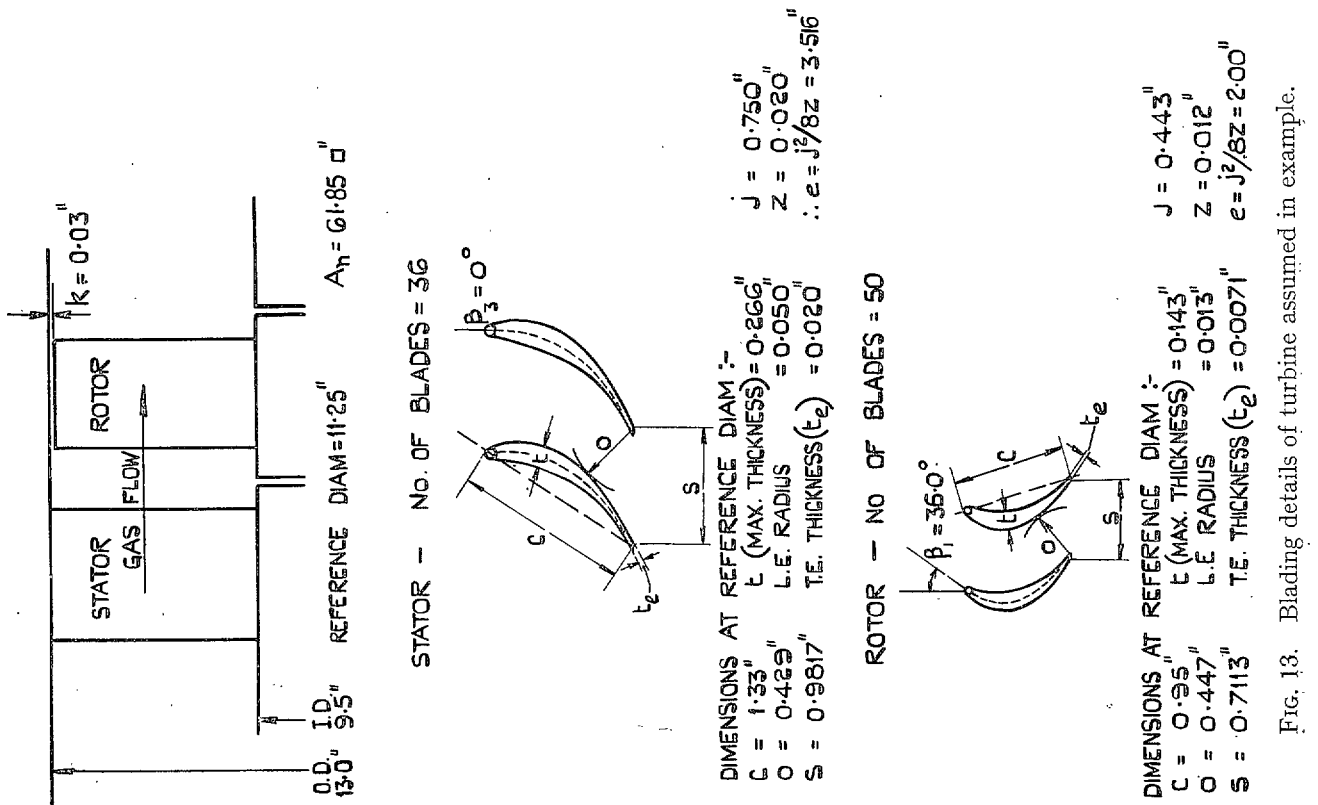
FIG. 12.   Compressible adiabatic flow.

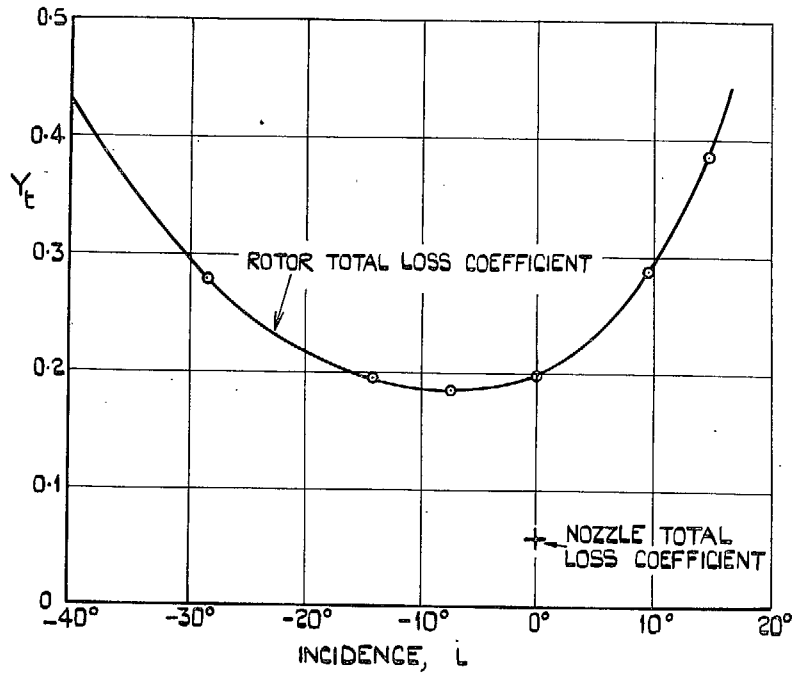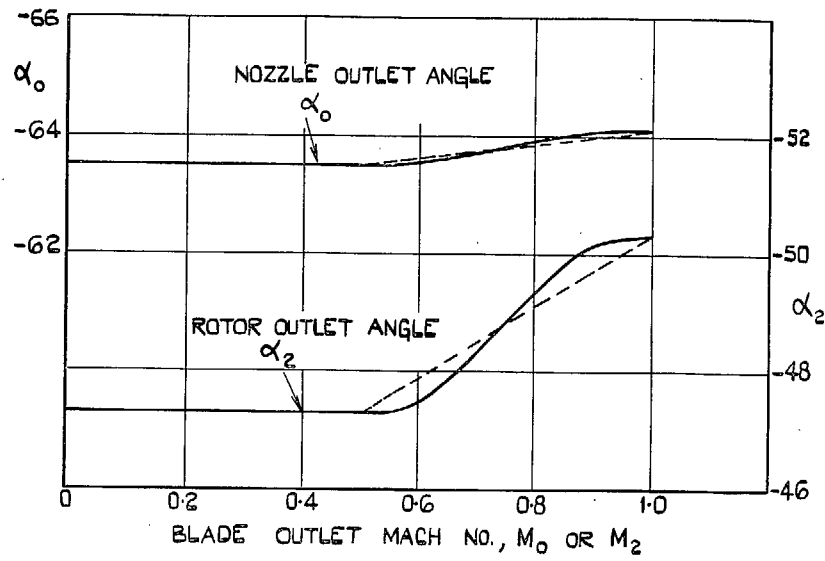FIG. 13.   Blading details of turbine assumed in example.

FIG. 14. Gas outlet angles and loss coefficients of turbine assumed in example.
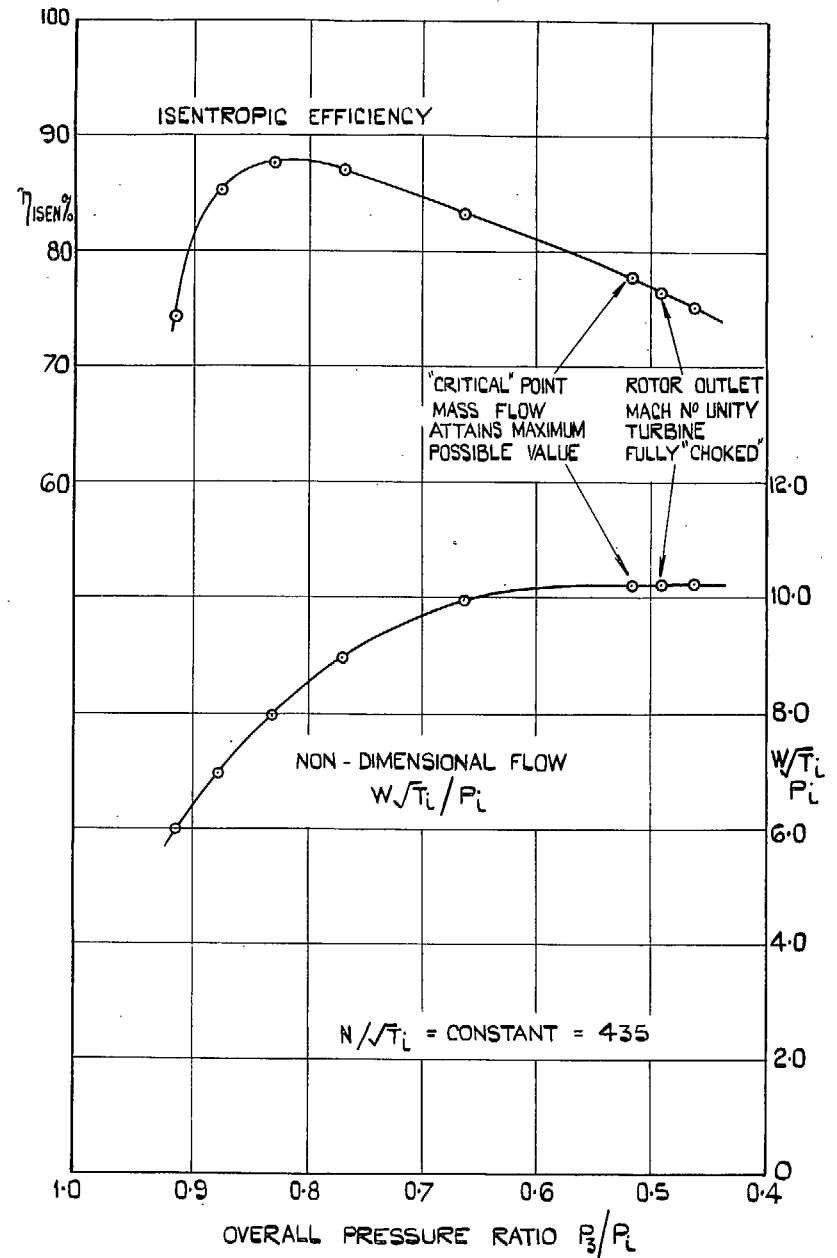

FIG. 15. Constant-speed characteristic (calculated) for turbine assumed in example.

CALCULATED PERFORMANCE OF A SINGLE STAGE TURBINE

$N/\sqrt{T_i} = 435$; $T_i = 1100°K$; $P_i = 40 \; p.s.i.a.$; $K_p = 12,300$ ft. pdl./lb/°C; $\gamma = 1.3330$

No.	Symbol										Notes
1	$W\sqrt{T_i}/P_i$	6.0	7.0	8.0	9.0	10.0	10.28	10.268			ARBITRARILY SELECTED
2	W LBS/SEC	7.24	8.44	9.65	10.86	12.07	12.40	12.386			FOR SELECTED VALUES OF P_i AND T_i
3	α_o	-63.50	-63.50	-63.50	-63.55	-63.90	-64.10	-63.05			APPROXIMATE VALUE (CONJECTURAL)
4	$W\sqrt{T_i}/P_i\,A_{no}\,\cos\alpha_o$	0.2176	0.254	0.290	0.327	0.368	0.3805	0.37947			DESIGNATED Q
5	ι (NOZZLE)	0	0	0	0	0	0	0			FROM INCIDENCE AND FIGURE 17 — SEE ALSO SECTION 6.2
6	Y_t (NOZZLE)	0.0583	0.0583	0.0583	0.0583	0.0583	0.0583	0.0583			FROM FIGURE 13 AND VALUE OF Y_t (NOZZLE)
7	Q MAX	0.3805	0.3805	0.3805	0.3805	0.3805	0.3805	0.3805			FROM FIGURE 14 AND VALUE OF Y_t (NOZZLE)
8	$(\bar\omega/P_i)_{CRIT}$	0.0253	0.0253	0.0253	0.0253	0.0253	0.0253	0.0253			FROM LINES 4 AND 7.
9	Q/Q MAX	0.571	0.668	0.762	0.859	0.966	1.00	0.9973			FROM FIGURE 15
10	$\bar\omega/\bar\omega$ CRIT	0.176	0.252	0.348	0.483	0.728	1.00	0.925			
11	$\bar\omega/P_i$	0.00445	0.00637	0.0088	0.0122	0.0184	0.0253	0.0234			FROM LINES 10 AND 8
12	$\bar\omega$	0.178	0.255	0.352	0.488	0.736	1.012	0.936			SINCE P_i = 40 LBS/SQ. IN ABSOLUTE
13	P_o	39.822	39.745	39.648	39.512	39.264	38.988	39.064			$P_i - \bar\omega$.
14	$W\sqrt{T_o}/P_o\,A_{no}\,\cos\alpha_o$	0.2185	0.2558	0.2925	0.331	0.3747	0.3901	0.38862			SINCE T_o = T_i
15	M_o	0.345	0.423	0.505	0.61	0.791	0.958	0.923			FROM FIGURE 11
16	α_o	-63.5	-63.5	-63.5	-63.51	-63.92	-64.1	-64.08			THIS SHOULD AGREE WITH VALUE ASSUMED IN LINE 3 TO WITHIN ±0.2° IF NOT STEPS 3 TO 16 MUST BE REWORKED WITH A CLOSER APPROXIMATION TO α_o.
17	$V_o/\sqrt{T_o}$	22.12	26.7	31.65	37.9	48.2	57.4	55.4			FROM FIGURE 12
18	V_o	773	885	1050	1257	1600	1902	1835			SINCE T_o = T_i = 1100 °K
19	V_{a1}	326.5	394.5	469	560	704	830	802			$V_o \cos\alpha_o$
20	U/V_{a1}	-2.165	-1.794	-1.51	-1.263	-1.005	-0.852	-0.883			U = -708 FT/SEC.
21	TAN α_o	-2.006	-2.006	-2.006	-2.009	-2.041	-2.059	-2.055			
22	TAN α_1	-0.159	0.212	0.496	0.746	1.036	1.207	1.172			TAN α_1 = U/V_{a1} - TAN α_o (EQUATION 8)
23	α_1	-9.05	12.0	26.4	36.75	46.0	50.35	49.5			
24	ι (ROTOR)	-45.05	-24.0	-9.6	0.75	10.0	14.35	13.5			ι (ROTOR) = α_1 - β_1
25	$T_o - T_i$	17.4	25.2	33.7	44.35	62.4	78.2	74.6			EQUATION 12
26	$(T_o - T_i)/T_o$	0.0158	0.0229	0.0306	0.0403	0.0567	0.0711	.0678			
27	$(P_o - P_i)/P_o$	0.0618	0.0883	0.1167	0.1517	0.2075	0.2550	0.2445			EQUATION 13
28	$(P_o - P_i)$	2.461	3.51	4.622	5.99	8.15	9.94	9.550.			
29	P_i	37.361	36.235	35.026	33.522	31.114	29.048	29.514	29.514	29.514	
30	T_i	1082.6	1074.8	1066.3	1055.65	1037.6	1021.8	1025.4	1025.4	1025.4	
31	α_2	-47.3	-47.3	-47.3	-47.3	-47.4	-50.1	-50.1			APPROXIMATE VALUE (CONJECTURAL)
32	$W\sqrt{T_i}/P_i\,A_{n2}\,\cos\alpha_2$	0.1522	0.1821	0.2145	0.251	0.299	0.3452	0.3387			DESIGNATED Q
33	Y_t (ROTOR)	0.510	0.240	0.188	0.203	0.295	0.385	0.360	0.360	0.360	FROM INCIDENCE (LINE 24) AND FIGURE 17
34	Q MAX	0.3223	0.3536	0.3605	0.3585	0.3465	0.3358	0.3387			FROM FIGURE 13 AND VALUE OF Y_t (ROTOR).
35	$(\bar\omega/P_i)_{CRIT}$	0.1590	0.090	0.0735	0.0785	0.1035		0.1235			FROM FIGURE 14 AND VALUE OF Y_t (ROTOR)
36	Q/Q MAX	0.472	0.515	0.595	0.700	0.863	>1.0	1.0			FROM LINES 32 AND 34
37	$\bar\omega/\bar\omega$ CRIT	0.117	0.141	0.194	0.282	0.490		1.0			FROM FIGURE 15 AND VALUE OF Q/Q MAX IN LINE 36.
38	$\bar\omega/P_i$	0.0186	0.0127	0.0143	0.0221	0.0507		0.1235			FROM LINES 35 AND 37
39	$\bar\omega$	0.695	0.460	0.500	0.741	1.578		3.642			
40	P_i	36.666	35.775	34.526	32.781	29.536		25.872			$P_i - \bar\omega$
41	$W\sqrt{T_i}/P_i\,A_{n2}\,\cos\alpha_2$	0.1550	0.1845	0.2180	0.2567	0.3150		0.3866			N.B. $T_2 = T_i$
42	M_2	0.239	0.289	0.349	0.425	0.563		0.892	1.0	1.15	FROM LINE 41 AND FIGURE 11. ARBITRARY VALUES SELECTED WHEN M_2 > M_2 CRIT
43	α_2	-47.3	-47.3	-47.3	-47.3	-47.31		-50.13			THIS VALUE SHOULD AGREE WITH VALUE ASSUMED IN LINE 31 WITHIN ±0.2° IF NOT STEPS 31 TO 43 MUST BE RECALCULATED WITH A CLOSER APPROXIMATION TO α_2.
44	p_2/P_2								0.540	0.4508	FROM FIGURE 10
45	$\bar\omega/P_2$								0.1656	0.1975	EQUATION 21 APPENDIX II
46	$\bar\omega/P_i$								0.1421	0.1650	$\bar\omega/P_2/(1 + \bar\omega/P_2)$
47	$\bar\omega$								4.200	4.870	
48	P_i								25.314	24.644	
49	$W\sqrt{T_2}/A_2 P_2$								0.3907	0.3837	FROM FIGURE 11 AND SELECTED VALUES OF M_2 IN LINE 42.
50	A_2								40.05	41.9	FROM LINE 49 AND KNOWN VALUES OF $W_1 T_2$ AND P_2
51	α_2								-49.6	-47.3	α_2 = - $\cos^{-1}(A_2/A_{n2})$
52	$V_2/\sqrt{T_2}$	15.21	18.38	22.08	26.80	35.14		53.80	59.26	66.70	FROM FIGURE 12
53	V_2	500.5	601	721.	870	1130		1720	1898	2137	
54	V_{a2}	340.0	408	489	590	765		1102	1230	1448	$V_2 \cos\alpha_2$
55	TAN α_2	-1.084	-1.084	-1.084	-1.084	-1.084		-1.196	-1.175	-1.084	
56	U/V_{a2}	-2.080	-1.735	-1.448	-1.200	-0.925		-0.642	-0.575	-0.489	
57	TAN α_3	-0.996	-0.651	-0.364	-0.116	0.159		0.554	0.600	0.595	TAN α_3 = U/V_{a2} - TAN α_2
58	α_3	-44.9	-33.1	-20.0	-6.6	9.0		29.0	31.0	30.8	
59	$T_2 - T_3$	0.845	5.05	10.11	16.41	27.45		55.7	62.8	69.8	FROM EQUATION 16
60	$(T_2 - T_3)/T_2$	0.00078	0.0047	0.0095	0.01557	0.02645		0.0543	0.0612	0.0681	
61	$(P_2 - P_3)/P_2$	0.00312	0.0187	0.0374	0.0608	0.1017		0.200	0.223	0.245	FROM EQUATION 18
62	$P_2 - P_3$	0.1143	0.668	1.291	1.991	3.000		5.174	5.645	6.040	
63	P_3	36.552	35.107	33.235	30.790	26.536		20.698	19.669	18.604	
64	T_3	1081.75	1069.75	1056.19	1039.24	1010.15		989.7	962.6	955.6	
65	$T_L - T_3 / T_L$	0.0166	0.0275	0.0398	0.0552	0.0817		0.1184	0.125	0.1312	
66	P_3/P_i	0.9138	0.8777	0.8309	0.7698	0.6634		0.5174	0.4917	0.4651	
67	$\Delta T_{ISEN}/T_L$	0.0223	0.0322	0.0452	0.0634	0.097G		0.1520	0.1625	0.1742	OVERALL VALUES OF NON-DIMENSIONAL TEMPERATURE DROP PRESSURE DROP EFFICIENCY, ETC
68	η_{ISEN}	0.745	0.855	0.880	0.8715	0.837		0.780	0.769	0.753	FOR STAGE.
69	$2K_p \Delta T/U^2$	0.896	1.485	2.15	2.98	4.41		6.41	6.75	7.1	
70	$W\sqrt{T_i}/P_i$	6.0	7.0	8.0	9.0	10.0		10.268	10.268	10.268	

Side section labels: NOZZLE INLET AND OUTLET; RELATIVE CONDITIONS INLET AND OUTLET TO ROTOR; RELATIVE ROTOR OUTLET CONDITIONS WHEN $M_2 > M_2$ CRIT; ABSOLUTE ROTOR OUTLET CONDITIONS; OVERALL STAGE CHARACTERISTICS.

FIG. 16.

Publications of the
Aeronautical Research Council

ANNUAL TECHNICAL REPORTS OF THE AERONAUTICAL RESEARCH COUNCIL (BOUND VOLUMES)

1939 Vol. I. Aerodynamics General, Performance, Airscrews, Engines. 50s. (51s. 9d.)
  Vol. II. Stability and Control, Flutter and Vibration, Instruments, Structures, Seaplanes, etc. 63s. (64s. 9d.)

1940 Aero and Hydrodynamics, Aerofoils, Airscrews, Engines, Flutter, Icing, Stability and Control, Structures, and a miscellaneous section. 50s. (51s. 9d.)

1941 Aero and Hydrodynamics, Aerofoils, Airscrews, Engines, Flutter, Stability and Control, Structures. 63s. (64s. 9d.)

1942 Vol. I. Aero and Hydrodynamics, Aerofoils, Airscrews, Engines. 75s. (76s. 9d.)
  Vol. II. Noise, Parachutes, Stability and Control, Structures, Vibration, Wind Tunnels. 47s. 6d. (49s. 3d.)

1943 Vol. I. Aerodynamics, Aerofoils, Airscrews. 80s. (81s. 9d.)
  Vol. II. Engines, Flutter, Materials, Parachutes, Performance, Stability and Control, Structures. 90s. (92s. 6d.)

1944 Vol. I. Aero and Hydrodynamics, Aerofoils, Aircraft, Airscrews, Controls. 84s. (86s. 3d.)
  Vol. II. Flutter and Vibration, Materials, Miscellaneous, Navigation, Parachutes, Performance, Plates and Panels, Stability, Structures, Test Equipment, Wind Tunnels. 84s. (86s. 3d.)

1945 Vol. I. Aero and Hydrodynamics, Aerofoils. 130s. (132s. 6d.)
  Vol. II. Aircraft, Airscrews, Controls. 130s. (132s. 6d.)
  Vol. III. Flutter and Vibration, Instruments, Miscellaneous, Parachutes, Plates and Panels, Propulsion. 130s (132s. 3d.)
  Vol. IV. Stability, Structures, Wind tunnels, Wind Tunnel Technique. 130s. (132s. 3d.)

ANNUAL REPORTS OF THE AERONAUTICAL RESEARCH COUNCIL—

1937 2s. (2s. 2d.)   1938 1s. 6d. (1s. 8d.)   1939–48 3s. (3s. 3d.)

INDEX TO ALL REPORTS AND MEMORANDA PUBLISHED IN THE ANNUAL TECHNICAL REPORTS, AND SEPARATELY—

April, 1950 – – – – – R. & M. No. 2600.   2s. 6d. (2s. 8d.)

AUTHOR INDEX TO ALL REPORTS AND MEMORANDA OF THE AERONAUTICAL RESEARCH COUNCIL—

1909–January, 1954 – – – R. & M. No. 2570.   15s. (15s. 6d.)

INDEXES TO THE TECHNICAL REPORTS OF THE AERONAUTICAL RESEARCH COUNCIL—

December 1, 1936 — June 30, 1939.   R. & M. No. 1850.   1s. 3d. (1s. 5d.)
July 1, 1939 — June 30, 1945.   –   R. & M. No. 1950.   1s. (1s. 2d.)
July 1, 1945 — June 30, 1946.   –   R. & M. No. 2050.   1s. (1s. 2d.)
July 1, 1946 — December 31, 1946.   R. & M. No. 2150.   1s. 3d. (1s. 5d.)
January 1, 1947 — June 30, 1947. –   R. & M. No. 2250.   1s. 3d. (1s. 5d.)

PUBLISHED REPORTS AND MEMORANDA OF THE AERONAUTICAL RESEARCH COUNCIL—

Between Nos. 2251–2349.   –   –   R. & M. No. 2350.   1s. 9d. (1s. 11d.)
Between Nos. 2351–2449.   –   –   R. & M. No. 2450.   2s. (2s. 2d.)
Between Nos. 2451–2549.   –   –   R. & M. No. 2550.   2s. 6d. (2s. 8d.)
Between Nos. 2551–2649.   –   –   R. & M. No. 2650.   2s. 6d. (2s. 8d.)

Prices in brackets include postage

HER MAJESTY'S STATIONERY OFFICE